# 75. Semileptonic $b$-Hadron Decays, Determination of $V_{cb}$, $V_{ub}$

Revised August 2019 by T. Mannel (Siegen U.) and P. Urquijo (School of Phys. U. of Melbourne).

## 75.1 Introduction

Precision determinations of $|V_{ub}|$ and $|V_{cb}|$ are central to testing the CKM sector of the Standard Model, and complement the measurements of CP asymmetries in $B$ decays. The length of the side of the unitarity triangle opposite the well-measured angle $\beta$ is proportional to the ratio $|V_{ub}|/|V_{cb}|$; its precise determination is a high priority of the heavy-flavor physics program.

The transitions $b \to c\ell\bar{\nu}_\ell$ and $b \to u\ell\bar{\nu}_\ell$ (where $\ell$ refers to an electron or muon) each provide two avenues for determining these CKM matrix elements, namely through inclusive (i.e. the sum over all possible hadronic states) and exclusive final states (decays involving a specific meson, $X = D$, $D^*$, $\pi$, $\rho$ etc.). While the purely leptonic final states in the decays $B_c^- \to \tau\bar{\nu}$, $B^- \to \tau\bar{\nu}$, and $B^- \to \mu\bar{\nu}$ are theoretically very simple, we do not use this information at present since none of the measurements has reached a competitive level of precision and thus the focus is on exclusive and inclusive semileptonic decays. This article and the values quoted here update the previous review [1].

The theory underlying the different determinations of $|V_{qb}|$ is mature, in particular for $|V_{cb}|$. Most of the theoretical approaches use the fact that the masses $m_b$ and $m_c$ of the $b$ and the $c$ quark are large compared to the scale $\Lambda_{\rm QCD}$ that determines low-energy hadronic physics. Thus the basis for precise calculations is a systematic expansion in powers of $\Lambda/m_b$, where $\Lambda \sim 500 - 700$ MeV is a hadronic scale of the order of $\Lambda_{\rm QCD}$. Such an expansion can be formulated in the framework of an effective field theory which is described in a separate RPP mini-review [2].

Aside from this there has been significant progress over the last decade in lattice simulations of QCD which is a first-principles method for non-perturbative QCD calculations. Increased computer power as well as improved theoretical methods allow us to include also heavy quarks in this calculations, and thus the results from lattice QCD play an essential role in many of the determinations discussed here. We do not need to describe lattice methods here, they are discussed in a separate RPP mini-review [3].

The measurements discussed in this review are of branching fractions, ratios of branching fractions, and decay kinematic distributions. The determinations of $|V_{cb}|$ and $|V_{ub}|$ also require a measurement of the total decay widths of the corresponding $b$ hadrons, determined from lifetimes, which is the subject of a separate RPP mini-review [4]. The measurements of inclusive semileptonic decays relevant to this review come primarily from $e^+e^-$ $B$ factories operating at the $\Upsilon(4S)$ resonance, while the measurements of exclusive semileptonic decays come from both the $e^+e^-$ $B$ factories and from the LHCb experiment at CERN.

Semileptonic B meson decay amplitudes to electrons and muons are well measuered and consistent with the SM, and thus are dominated by the Standard-Model $W$ boson exchange, which is expected to be largely free from any impact of non-Standard Model physics. The decays $\bar{B} \to D^{(*)}\tau\bar{\nu}_\tau$, however, may become sensitive to effects beyond the Standard Model due to the large masss of the $\tau$ lepton. For example, modifications in the Higgs sector such as a charged Higgs boson, may couple to the mass of the leptons, breaking lepton universality beyond the Standard Model. The currently observed anomalies in these decay could be an indication of new physics.

Many of the numerical results quoted in this review have been provided by the Heavy Flavor Averaging Group (HFLAV) [5].

## 75.2 Determination of $|V_{cb}|$

*Summary:* The determination of $|V_{cb}|$ from inclusive decays has a relative uncertainty of about 2%; the limitations arise mainly from our ignorance of higher-order perturbative and non-perturbative corrections. Exclusive $\bar{B} \to D^* \ell \bar{\nu}_\ell$ decays provide a determination of $|V_{cb}|$ with a relative precision of about 2%, with comparable contributions from theory and experiment; the value determined from $\bar{B} \to D \ell \bar{\nu}_\ell$ decays is consistent and has an uncertainty of 3%. However, as discussed below, recent work has raised questions about these determinations. We choose to quote a less constraining value from exclusive decays.

The values obtained from the inclusive and exclusive determinations discussed below are:

$$|V_{cb}| = (42.2 \pm 0.8) \times 10^{-3} \quad \text{(inclusive)} \tag{75.1}$$

$$|V_{cb}| = (39.5 \pm 0.9) \times 10^{-3} \quad \text{(exclusive)}. \tag{75.2}$$

An average of these determinations has $p(\chi^2) = 2\%$, so we scale the error by $\sqrt{\chi^2/1} = 2.4$ to find

$$|V_{cb}| = (41.0 \pm 1.4) \times 10^{-3} \quad \text{(average)}. \tag{75.3}$$

Given the only marginal consistency this average should be treated with caution.

### 75.2.1 $|V_{cb}|$ *from exclusive decays*

Exclusive determinations of $|V_{cb}|$ make use of semileptonic $B$ decays into the ground state charmed mesons $D$ and $D^*$. Based on Lorentz-invariance these decays are collectively described in terms of six independent form factors, which depend on the variable $w \equiv v \cdot v'$, where $v$ and $v'$ are the four velocities of the initial and final-state hadrons. In the rest frame of the decay this variable corresponds to the Lorentz factor of the final state $D^{(*)}$ meson. Heavy Quark Symmetry (HQS) [6] [7] predicts that in the infinite mass limit the six form factors collapse into a single one, which is normalized at the "zero recoil point" $w = 1$, the point of maximum momentum transfer to the leptons.

The determination of $|V_{cb}|$ requires a calculation of the form factors. One possibility is to use the normalization of the form factor at $w = 1$, however, a precise determination requires to include corrections to the HQS prediction for the normalization as well as some information on the shape of the form factors near the point $w = 1$. These calculations utilize Heavy Quark Effective Theory, which is discussed in a separate RPP mini-review [2]. Some of the form factors are normalized at $w = 1$ due to HQS, and this normalization is protected against linear corrections [8], and thus the leading corrections to the normalization are of order $\Lambda^2_{\rm QCD}/m_c^2$. For the form factors that vanish in the infinite mass limit the corrections are in general linear in $\Lambda_{\rm QCD}/m_c$.

In addition to these corrections, there are perturbatively calculable corrections from hard gluons as well as QED radiative corrections, which will be discussed in the relevant sections.

### 75.2.2 $\bar{B} \to D^* \ell \bar{\nu}_\ell$

The decay rate for $\bar{B} \to D^* \ell \bar{\nu}_\ell$ is given by

$$\frac{d\Gamma}{dw}(\bar{B} \to D^* \ell \bar{\nu}_\ell) = \frac{G_F^2 m_B^5}{48\pi^3} |V_{cb}|^2 (w^2-1)^{1/2} P(w) (\eta_{\rm ew} \mathcal{F}(w))^2, \tag{75.4}$$

where $P(w)$ is a phase space factor,

$$P(w) = r^3 (1-r)^2 (w+1)^2 \left(1 + \frac{4w}{w+1} \frac{1-2rw+r^2}{(1-r)^2}\right). \tag{75.5}$$

with $r = m_{D^*}/m_B$. The form factor $\mathcal{F}(w)$ can be expressed in terms of the vector and axial vector form factors

$$\frac{\langle D^*(v',\epsilon)|\bar{c}\gamma^\mu b|B(v)\rangle}{\sqrt{m_B m_{D^*}}} = h_V(w)\,\varepsilon^{\mu\nu\rho\sigma} v_{B,\nu} v_{D^*,\rho} \epsilon^*_\sigma, \tag{75.6}$$
$$\frac{\langle D^*(v',\epsilon)|\bar{c}\gamma^\mu\gamma^5 b|B(v)\rangle}{\sqrt{m_B m_{D^*}}} = i h_{A_1}(w)\,(1+w)\epsilon^{*\mu} - i\,[h_{A_2}(w) v_B^\mu + h_{A_3}(w) v_{D^*}^\mu]\,\epsilon^*\cdot v_B$$

as

$$P(w)|\mathcal{F}(w)|^2 = |h_{A_1}(w)|^2 \left\{ 2\frac{r^2 - 2rw + 1}{(1-r)^2}\left[1 + \frac{w-1}{w+1} R_1^2(w)\right] \right. \tag{75.7}$$
$$\left. + \left[1 + \frac{w-1}{1-r}(1 - R_2(w))\right]^2 \right\},$$

where the ratios $R_1$ and $R_2$ are given by

$$R_1(w) = \frac{h_V(w)}{h_{A_1}(w)}, \quad R_2(w) = \frac{h_{A_3}(w) + r\,h_{A_2}(w)}{h_{A_1}(w)}. \tag{75.8}$$

Note that $\mathcal{F}$ at $w = 1$ is unity by HQS in the infinite-mass limit [9–12]. Usually the decay rate formulae for semileptonic $B$ decays assume massless leptons. The effect is typically very small, but for the muon case can be non-negligible in fits to data at high hadronic recoil.

The factor $\eta_{\rm ew} = 1.0066 \pm 0.0050$ accounts for the leading electroweak corrections to the four-fermion operator mediating the semileptonic decay [13], and includes an estimated uncertainty for missing long-distance QED radiative corrections [14].

The determination of $V_{cb}$ using the normalization at $w = 1$ involves an extrapolation to the zero-recoil point, for which a parametrization of the shape of $\mathcal{F}(w)$ is needed. Convenient parametrizations make use of analyticity and unitarity constraints on the the form factors and are expressed in terms of the variable

$$z = (\sqrt{w+1} - \sqrt{2})/(\sqrt{w+1} + \sqrt{2}), \tag{75.9}$$

originating from a conformal transformation. In terms of this variable the form factors (generically denoted as $F$) may be written as [15–17]

$$F(z) = \frac{1}{P_F(z)\phi_F(z)} \sum_{n=0}^{\infty} a_n z^n \tag{75.10}$$

where the sum is bounded, $\sum |a_n|^2 < 1$. Furthermore, the function $P_F(z)$ takes into account the resonances in the $(\bar{c}b)$ system below the $\bar{D}B$ threshold, and the weighting functions $\phi_F(z)$ are derived from the unitarity constraint on the corresponding form factor. The values of $z$ relevant to the decay are $0 \le z \le 0.06$, hence only very few terms are needed in the series in $z$. Eq. (75.10) will be referred to as the "BGL" expansion.

A frequently used parametrization proposed in Ref. [18] is a simple one-parameter form

$$h_{A_1}(w) = h_{A_1}(1)\left[1 - 8\rho^2 z + (53\rho^2 - 15)z^2 + (231\rho^2 - 91)z^3\right] \tag{75.11}$$

which has the slope $\rho$ and of the form factor and the value $h_{A_1}(1)$ as the only parameters. Furthermore, the ratios $R_1(w)$ and $R_1(w)$ are expanded in $w - 1$. However, this simple CLN parametrtization is inconsistent in subleading orders of the $1/m_{c/b}$ expansion [17, 19–22], and thus the recent

fits are based on the BGL expansion. Typical fits include up to three parameters $a_n$ in (75.10) for the different form factors.

The theoretical analysis of $F(w)$ requires, aside from the perturbative calculation of QCD short-distance radiative correction [23], the treatment of non-perturbative aspects. The state-of-the-art input comes from lattice QCD calculations which include a realistic description of the sea quarks using $2+1$ or $2+1+1$ flavors and finite $b$ and $c$ masses.

Currently available are lattice results only for the value $\mathcal{F}(1)$ at the non-recoil point [14,24] with a total uncertainty at the (1-2)% level. The main contributions to this uncertainty in case of the Fermilab/MILC calculation are from the chiral extrapolation from the light quark masses used in the numerical lattice computation to realistic up and down quark masses, and from discretization errors. In the HPQCD calculation, the dominant source of uncertainty is the perturbative matching calculation for the heavy-light currents. These sources of uncertainty will be reduced with larger lattice sizes and smaller lattice spacings. The average of the two lattice predictions [25] is

$$\mathcal{F}(1) = 0.904 \pm 0.012, \tag{75.12}$$

Lattice calculations for values of $F(w)$ for $w \neq 1$ are underway, but not yet available.

Non-lattice estimates based on zero-recoil sum rules for the form factor tend to yield lower central values for $\mathcal{F}(1)$ [26–28]. Omitting the contributions from excited states, the sum rules indicate that $\mathcal{F}(1) < 0.93$. Including an estimate for the contribution of the excited states yields $\mathcal{F}(1) = 0.86 \pm 0.01 \pm 0.02$ [28,29] where the second uncertainty accounts for the excited states.

Many experiments [30–40] have measured the differential decay rate as a function of $w$, employing a variety of methods: using either $B^+$ or $B^0$ decays, with or without $B$-tagging, and with or without explicit reconstruction of the transition pion from $D^* \to D$ decays. These measurements are input to a four-dimensional fit [5] for $\eta_{\rm ew}\mathcal{F}(1)|V_{cb}|$, $\rho^2_{A_1}$ and the form-factor ratios $R_1 \propto A_2/A_1$ and $R_2 \propto V/A_1$. The fit has a $p$-value of 0.8%, so we scale the uncertainty by a factor $\sqrt{\chi^2/23}$ to give $\eta_{\rm ew}\mathcal{F}(1)\,|V_{cb}| = (35.27 \pm 0.52) \times 10^{-3}$ (CLN).

The leading sources of uncertainty on $\eta_{\rm ew}\mathcal{F}(1)\,|V_{cb}|$ are due to detection efficiencies and $D^{(*)}$ decay branching fractions. Note that the $\bar{B} \to D^*\ell\bar{\nu}_\ell$ form factor in the fit is parameterized using the CLN form, which has the drawbacks discussed previously.

Using the value from Eq. 75.12 for $\mathcal{F}(1)$ and accounting for the electroweak correction gives

$$|V_{cb}| = (38.8 \pm 0.6 \pm 0.6) \times 10^{-3}\ (\bar{B} \to D^*\ell\bar{\nu}_\ell,\ \text{LQCD, CLN}). \tag{75.13}$$

Not yet included in the average is the most recent measurement from Babar [41], which finds consistent results using the CLN form.

A safer approach is to use the more general BGL form-factor parameterization [17,19]. Two experiments have recently published analyses with BGL based parametrizations at a given order in the expansion [40,41]. The Belle analysis [40] is based on an untagged approach in the mode $\bar{B}^0 \to D^{*+}\ell\bar{\nu}_\ell$ and measures 1-$d$ projections in bins of the hadronic recoil $w$, and angular variables $\cos\theta_\ell$, $\cos\theta_V$, and $\chi$. The Babar analysis [41] is based on a hadronic tagged sample, and performs a full 4-$d$ unbinned analysis of neutral and charged $B$ decay modes. Only the BGL form factors are fit in this anlaysis, not the normalisation, which based on the world average $\bar{B} \to D^*\ell\bar{\nu}_\ell$ branching fraction.

At present only Ref. [40] publishes the fully-differential decay rate data and associated covariance matrix. An earlier preliminary measurement by Belle [39] also provided fully-differential decay rate data, used in a number of phenomenology analyses [17,19], but was not published.

The BGL fit results from Ref. [40], $|V_{cb}| = (38.4 \pm 1.0) \times 10^{-3}$, and Ref. [41], $|V_{cb}| = (38.4 \pm 0.9) \times 10^{-3}$, are consistent with result from the fit with the CLN parametrization, Eq. 75.13. Both

studies report fit results at low order in the three BGL expansion terms, ranging from zero-order to second-order in the Belle analysis, and first order for all terms in the Babar analysis. Studies of the impact of higher order expansions based on the Belle published decay rate data have been reported in Refs. [20,21], where it is shown that the fit uncertainty on $|V_{cb}|$ increases by approximately 50% with respect to the results reported at lower order. This is due to larger number of degrees of freedom allowed in the higher order expansions, however beyond second order there is very little information gain with the current measurements. Form-factor ratios are found to be consistent with HQET predictions based on fits to the published measurements. Without a combination of the two results at this stage, we choose to quote the arithmetic average of the results from Ref. [40, 41], where the central values are the same. The nominal result for $|V_{cb}|$ is therefore

$$|V_{cb}| = (38.4 \pm 0.7 \pm 0.5 \pm 1.0) \times 10^{-3} \ (\bar{B} \to D^* \ell \bar{\nu}_\ell, \ \text{LQCD, BGL}), \tag{75.14}$$

where the first uncertainty is experimental, the second is from LQCD, and the third is an additional uncertainty added by the authors to compensate for higher order expansion terms in the fit. Lattice QCD results for form factors away from zero recoil will be essential to control higher order terms in the BGL fit.

### 75.2.3 $\bar{B} \to D\ell\bar{\nu}_\ell$

The differential rate for $\bar{B} \to D\ell\bar{\nu}_\ell$ is given by

$$\frac{d\Gamma}{dw}(\bar{B} \to D\ell\bar{\nu}_\ell) = \\ \frac{G_F^2}{48\pi^3}|V_{cb}|^2(m_B + m_D)^2 m_D^3 (w^2-1)^{3/2}(\eta_{\rm ew}\mathcal{G}(w))^2. \tag{75.15}$$

The form factor is defined in terms of

$$\frac{\langle D(v')|\bar{c}\gamma^\mu b|B(v)\rangle}{\sqrt{m_B m_D}} = h_+(w)\,(v_B + v_D)^\mu + \, h_-(w)\,(v_B - v_D)^\mu \tag{75.16}$$

and reads

$$\mathcal{G}(w) = h_+(w) - \frac{m_B - m_D}{m_B + m_D} h_-(w), \tag{75.17}$$

where $h_+$ is normalized to unity due to HQS and $h_-$ vanishes in the infinite-mass limit. Thus

$$\mathcal{G}(1) = 1 + \mathcal{O}\left(\left(\frac{m_B - m_D}{m_B + m_D}\right)^2 \frac{\Lambda_{\rm QCD}}{m_c}\right) \tag{75.18}$$

and the corrections to the HQET predictions are of order $1/m$in contrast to the case of F (1).

The normalization, $\mathcal{G}(1)$, is obtained from QCD lattice calculations with realistic sea quarks and finite $b$ and $c$ masses. The most recent value for $\mathcal{G}(1)$ is derived in Ref. [42] and is

$$\mathcal{G}(1) = 1.054 \pm 0.004 \pm 0.008 \tag{75.19}$$

Based on a parametrization of the shape of $\mathcal{G}(w)$ a value of $|V_{cb}|$ can be extracted. However, $w \sim 1$ is a region with poor experimental precision given the low decay rate in this kinematic corner.

In fact, lattice calculations for the form factor $\mathcal{G}(w)$ (including sea quarks and finite $b$ and $c$ masses) are now available for values $w \neq 1$, thus providing information over a range of $z$ values (see Eq. (75.9)) [42,43]. This lattice input can be used in a simultaneous fit, along with the differential branching fraction, in a form-factor expansion in $z$ [15–17, 44].

The most precise measurements of $\bar{B} \to D\ell\bar{\nu}_\ell$ [37, 45, 46] dominate the CLN average [5] value, $\eta_{\rm ew}\mathcal{G}(1)|V_{cb}| = (42.00 \pm 1.00) \times 10^{-3}$. Note that this average corresponds to measurements that are fit to the CLN form factor parameterization; the same concerns expressed above for $\bar{B} \to D^*\ell\bar{\nu}_\ell$ apply here. Using the value from Eq. (75.19) for $\mathcal{G}(1)$ and accounting for the electroweak correction as above gives

$$|V_{cb}| = (39.6 \pm 0.9 \pm 0.3) \times 10^{-3} \quad (\bar{B} \to D\ell\bar{\nu}_\ell,\ \text{LQCD}, \text{CLN}), \tag{75.20}$$

where the first uncertainty is from experiment, and the second is from lattice QCD, as well as the electroweak corrections.

Studies have also been conducted using the general BCL form-factor parametrization ($z$-expansion from Ref. Ref. [44]), combining binned measurements from Belle [46] and Babar [45] with lattice QCD determinations of the form factors as a function of the recoil parameter in the lowest third of the kinematically allowed region [25]. Only Ref. [46] published the full measurement covariance matrix, while Ref. [45] provides the statistical uncertainty covariance. Nevertheless, Ref. [46] is more precise and dominates the average [25], giving

$$|V_{cb}| = (40.1 \pm 1.0) \times 10^{-3} \quad (\bar{B} \to D\ell\bar{\nu}_\ell,\ \text{LQCD}, \text{BCL}). \tag{75.21}$$

This result is consistent with the value reported in Ref. [47].

The $|V_{cb}|$ averages from $\bar{B} \to D^*\ell\bar{\nu}_\ell$ and $\bar{B} \to D\ell\bar{\nu}_\ell$ decays using the BGL and BCL forms, respectively, are reasonably consistent. The correlations between the lattice uncertainties for $\bar{B} \to D^*\ell\bar{\nu}_\ell$ and $\bar{B} \to D\ell\bar{\nu}_\ell$ are discussed in Ref. [25], and considered to be 100% for the statistical uncertainty component. We assume an experimental uncertainty correlation of order 20% and combine the results, giving

$$|V_{cb}| = (39.5 \pm 0.9) \times 10^{-3} \quad (\text{exclusive}). \tag{75.22}$$

### 75.2.4 $|V_{cb}|$ *from inclusive decays*

Measurements of the total semileptonic branching decay rate, along with moments of the lepton energy and hadronic invariant mass spectra in inclusive semileptonic $b \to c$ transitions, can be used for a precision determination of $|V_{cb}|$. The total semileptonic decay rate can be calculated quite reliably in terms of non-perturbative parameters that can be extracted from the information contained in the moments.

### 75.2.5 *Inclusive semileptonic rate*

The theoretical foundation for the calculation of the total semileptonic rate is the Operator Product Expansion (OPE) which yields the Heavy Quark Expansion (HQE) [48, 49]. Details can be found in the RPP mini-review on Effective Theories [2].

The OPE result for the total rate can be written schematically (details can be found, *e.g.*, in Ref. [50]) as

$$
\begin{aligned}
\Gamma = & |V_{cb}|^2 \frac{G_F^2 m_b^5(\mu)}{192\pi^3} \eta_{\rm ew} \times \\
& \left[ z_0^{(0)}(r) + \frac{\alpha_s(\mu)}{\pi} z_0^{(1)}(r) + \left(\frac{\alpha_s(\mu)}{\pi}\right)^2 z_0^{(2)}(r) + \cdots \right. \\
& + \frac{\mu_\pi^2}{m_b^2} \left( z_2^{(0)}(r) + \frac{\alpha_s(\mu)}{\pi} z_2^{(1)}(r) + \cdots \right) \\
& + \frac{\mu_G^2}{m_b^2} \left( y_2^{(0)}(r) + \frac{\alpha_s(\mu)}{\pi} y_2^{(1)}(r) + \cdots \right) \\
& + \frac{\rho_{\rm D}^3}{m_b^3} \left( z_3^{(0)}(r) + \frac{\alpha_s(\mu)}{\pi} z_3^{(1)}(r) + \cdots \right) \\
& \left. + \frac{\rho_{\rm LS}^3}{m_b^3} \left( y_3^{(0)}(r) + \frac{\alpha_s(\mu)}{\pi} y_3^{(1)}(r) + \cdots \right) + ... \right]
\end{aligned}
\tag{75.23}
$$

where $r$ is the ratio $m_c/m_b$ and the $y_i$ and $z_i$ are perturbatively calculable Wilson coefficients functions that appear at different orders of the heavy mass expansion.

The parameters $\mu_\pi$, $\mu_G$, $\rho_D$ and $\rho_{LS}$ constitute the non-perturbative input into the heavy quark expansion; they correspond to certain matrix elements to be discussed below. In the same way the HQE can be set up for the moments of distributions of charged-lepton energy, hadronic invariant mass and hadronic energy, e.g.

$$
\langle E_e^n \rangle_{E_e > E_{\rm cut}} = \int_{E_{\rm cut}}^{E_{\rm max}} \frac{d\Gamma}{dE_e} E_e^n dE_e \Bigg/ \int_{E_{\rm cut}}^{E_{\rm max}} \frac{d\Gamma}{dE_e} dE_e \, . \tag{75.24}
$$

The coefficients of the HQE are known up to order $1/m_b^5$ at tree level [51–54]. The leading term $z_0^{(i)}$ is the parton model, and is known completely to order $\alpha_s$ and $\alpha_s^2$ [55–57]. The terms of order $\alpha_s^{n+1}\beta_0^n$ (where $\beta_0$ is the first coefficient of the QCD $\beta$ function, $\beta_0 = (33 - 2n_f)/3$) have been included by the usual BLM procedure [50, 58, 59]. Corrections of order $\alpha_s \mu_\pi^2/m_b^2$ have been computed in Ref. [60] and Ref. [61], while the $\alpha_s \mu_G^2/m_b^2$ terms have been calculated in Ref. [62] and Ref. [63].

Starting at order $1/m_b^3$ contributions with an infrared sensitivity to the charm mass, $m_c$, appear [51, 53, 64, 65]. At order $1/m_b^3$ this "intrinsic charm" contribution manifests as a $\log(m_c)$ in the coefficient of the Darwin term $\rho_D^3$. At higher orders, terms such as $1/m_b^3 \times 1/m_c^2$ and $\alpha_s(m_c) 1/m_b^3 \times 1/m_c$ appear, which are comparable in size to the contributions of order $1/m_b^4$.

The HQE parameters are given in terms of forward matrix elements of local operators; the parameters entering the expansion for orders up to $1/m_b^3$ are ($D_\perp^\mu = (g_{\mu\nu} - v_\mu v_\nu) D^\nu$, where $v = p_B/M_B$ is the four-velocity of the $B$ meson)

$$
\begin{aligned}
\overline{\Lambda} &= M_B - m_b \, , \\
\mu_\pi^2 &= -\langle B|\bar{b}(iD_\perp)^2 b|B\rangle \, , \\
\mu_G^2 &= \langle B|\bar{b}(iD_\perp^\mu)(iD_\perp^\nu)\sigma_{\mu\nu} b|B\rangle \, , \\
\rho_{\rm D}^3 &= \langle B|\bar{b}(iD_{\perp\mu})(ivD)(iD_\perp^\nu) b|B\rangle \, , \\
\rho_{\rm LS}^3 &= \langle B|\bar{b}(iD_\perp^\mu)(ivD)(iD_\perp^\nu)\sigma_{\mu\nu} b|B\rangle .
\end{aligned}
\tag{75.25}
$$

These parameters still depend on the heavy quark mass. Sometimes the infinite mass limits of these parameters $\overline{\Lambda} \to \overline{\Lambda}_{\rm HQET}$, $\mu_\pi^2 \to -\lambda_1$, $\mu_G^2 \to 3\lambda_2$, $\rho_D^3 \to \rho_1$ and $\rho_{LS}^3 \to 3\rho_2$, are used instead. Beyond

$1/m^3$ the number of independent HQE parameters starts to proliferate [66]. In general, there are 13 parameters (at tree level) up to order $1/m^4$ and 31 (at tree level) up to order $1/m^5$, not including $\overline{\Lambda}$ . The HQE parameters of the orders $1/m_b^4$ and $1/m_b^5$ have been estimated in Ref. [54,67], their impact on the $|V_{cb}|$ determination has been studied in Ref. [68]. However, it has been pointed out recently that one may reduce the number of independent parameters in the HQE by exploiting reparametrization invariance, which is a symmetry of the HQE stemming from Lorentz invariance of QCD [69]. For a subset of observables this allows us to reduce the number of parameters to three up to order $1/m^3$ ($\rho_{LS}$ can be absorbed into $\mu_G^2$ by a re-definition) and to 8 up to order $1/m^4$ [70].

The rates and the spectra depend strongly on the definition $m_b$ (or equivalently of $\overline{\Lambda}$). This makes the discussion of renormalization issues mandatory, since the size of QCD corrections is strongly correlated with the definitions used for the quark masses. For example, it is well known (see eg. [71]) that using the pole mass definition for heavy quark masses leads to a perturbative series for the decay rates that does not converge very well.

This motivates the use of "short-distance" mass definitions, such as the kinetic scheme [26] or the $1S$ scheme [72–74]. Both schemes are well suited for the HQE, since they allow the choice of the renormalization scale $\mu \leq m_b$. Furthermore, they both can be extracted from other observables to a sufficient precision, such that a precise determination of $|V_{cb}|$ becomes possible, despite of the strong quark-mass dependence of the total rate.

The $1S$ scheme eliminates the $b$ quark pole mass by relating it to the perturbative expression for the mass of the 1S state of the $\Upsilon$ system. The $b$ quark mass in the $1S$ scheme is is half of the perturbatively calculated mass of the 1S state of the $\Upsilon$ system. The best determination of the $b$ quark mass in the $1S$ scheme is obtained from sum rules for $e^+e^- \to b\bar{b}$ [75].

A second alternative is the so-called "kinetic mass" $m_b^{\rm kin}(\mu)$, which is the mass entering the non-relativistic expression for the kinetic energy of a heavy quark, and which is defined using heavy-quark sum rules [26].

### 75.2.6 *Determination of HQE Parameters and $|V_{cb}|$*

Several experiments have measured moments in $\bar{B} \to X_c \ell \bar{\nu}_\ell$ decays [76–84] as a function of the minimum lepton momentum. The measurements of the moments of the electron energy spectrum ($0^{\rm th}$-$3^{\rm rd}$) and of the squared hadronic mass spectrum ($0^{\rm th}$-$2^{\rm nd}$) have statistical uncertainties that are roughly equal to their systematic uncertainties. The $3^{\rm rd}$ order hadronic mass spectrum moments have also been measured by some experiments, with relatively large statistical uncertainty. The sets of moments measured within each experiment have strong correlations; their use in a global fit requires fully specified statistical and systematic covariance matrices. Measurements of photon energy moments ($0^{\rm th}$-$2^{\rm nd}$) in $B \to X_s\gamma$ decays [85–89] as a function of the minimum accepted photon energy are also used in some fits; the dominant uncertainties on these measurements are statistical.

Global fits [84,86,90–95]to the full set of moments have been performed in the 1S and kinetic schemes. The semileptonic moments alone determine a linear combination of $m_b$ and $m_c$ very accurately but leave the orthogonal combination poorly determined (See e.g. [96]); additional input is required to allow a precise determination of $m_b$. This additional information can come from the radiative $B \to X_s\gamma$ moments (with the caveat that the OPE for $b \to s\gamma$ breaks down beyond leading order in $\Lambda_{\rm QCD}/m_b$), which provide complementary information on $m_b$ and $\mu_\pi^2$, or from precise determinations of the charm quark mass [97,98]. The values obtained in the kinetic scheme fits [5,94,95] with these two constraints are consistent. Based on the charm quark mass constraint

$m_c^{\overline{\rm MS}}(3\,{\rm GeV}) = 0.986 \pm 0.013\,{\rm GeV}$ [99], a fit in the kinetic scheme [5] obtains

$$|V_{cb}| = (42.19 \pm 0.78) \times 10^{-3} \tag{75.26}$$

$$m_b^{\rm kin} = 4.554 \pm 0.018\,{\rm GeV} \tag{75.27}$$

$$\mu_\pi^2({\rm kin}) = 0.464 \pm 0.076\,{\rm GeV}^2, \tag{75.28}$$

where the errors include experimental and theoretical uncertainties. Theoretical uncertainties from higher orders in $1/m$ as well as in $\alpha_s$ are estimated and included in performing the fits. Similar values for the parameters are obtained with a variety of assumptions about the theoretical uncertainties and their correlations. The $\chi^2$/dof is well below unity in all fits, which could suggest that the theoretical uncertainties may be overestimated. However, while one could obtain a satisfactory fit with smaller uncertainties, this would result in unrealistically small uncertainties on the extracted HQE parameters, which are used as input to other calculations (e.g. the determination of $|V_{ub}|$). The mass in the $\overline{\rm MS}$ scheme corresponding to Eq. (75.27) is $m_b^{\overline{\rm MS}} = 4.19 \pm 0.04\,{\rm GeV}$, where the uncertainty includes a contribution from the translation between mass schemes; this can be compared with a value obtained using relativistic sum rules [99], $m_b^{\overline{\rm MS}} = 4.163 \pm 0.016\,{\rm GeV}$, which provides a non-trivial cross-check.

A fit to the measured moments in the 1S scheme [5, 86, 93] gives

$$|V_{cb}| = (41.98 \pm 0.45) \times 10^{-3} \tag{75.29}$$

$$m_b^{\rm 1S} = 4.691 \pm 0.037\,{\rm GeV} \tag{75.30}$$

$$\lambda_1({\rm 1S}) = -0.362 \pm 0.067\,{\rm GeV}^2, \tag{75.31}$$

This fit uses moments measurements from semileptonic and radiative decays and constrains the chromomagnetic operator using the $B^*$-$B$ and $D^*$-$D$ mass differences, but does not include the constraint on $m_c$ nor the full NNLO corrections.

The fits in the two renormalization schemes give consistent results for $|V_{cb}|$ and, after translation to a common renormalization scheme, for $m_b$ and $\mu_\pi^2$. We take the fit in the kinetic scheme [95], which includes higher-order corrections and results in a more conservative uncertainty, as the inclusive determination of $|V_{cb}|$:

$$|V_{cb}| = (42.2 \pm 0.8) \times 10^{-3}\ \text{(inclusive)}. \tag{75.32}$$

The precision of the global fit results can be further improved by calculating higher-order perturbative corrections to the coefficients of the HQE parameters. The inclusion of still-higher-order moments, if they can be measured with the required precision, may improve the sensitivity of the fits to higher-order terms in the HQE.

## 75.3 Determination of $|V_{ub}|$

*Summary:* Currently the best determinations of $|V_{ub}|$ are from $\bar{B} \to \pi \ell \bar{\nu}_\ell$ decays, where combined fits to theory and experimental data as a function of $q^2$ provide a precision of about 4%; the uncertainties from experiment and theory are comparable in size. Determinations based on inclusive semileptonic decays are based on different observables and use different strategies to suppress the $b \to c$ background. Most of the determinations are consistent and provide a precision of about 7%, with comparable contributions to the uncertainty from experiment and theory. The exception is the most recent Babar analysis, which observes significant model dependence.

The values obtained from inclusive and exclusive determinations are

$$|V_{ub}| = (4.25 \pm 0.12\ ^{+\ 0.15}_{-\ 0.14} \pm 0.23) \times 10^{-3} \quad \text{(inclusive)}, \tag{75.33}$$

$$|V_{ub}| = (3.70 \pm 0.10 \pm 0.12) \times 10^{-3} \quad \text{(exclusive)}, \tag{75.34}$$

where the last uncertainty on the inclusive result was added by the authors of this review and is discussed below.

The exclusive and inclusive determinations are independent, and the dominant uncertainties are on multiplicative factors.

To combine these values, the inclusive and exclusive values are weighted by their relative errors and the uncertainties are treated as normally distributed. The resulting average has $p(\chi^2) = 10\%$, so we scale the error by $\sqrt{\chi^2/1} = 1.6$ to find

$$|V_{ub}| = (3.82 \pm 0.24) \times 10^{-3} \quad \text{(average)}. \tag{75.35}$$

Given the somewhat poor consistency between the two determinations, this average should be treated with caution.

### 75.3.1 $|V_{ub}|$ *from inclusive decays*

The theoretical description of inclusive $\bar{B} \to X_u \ell \bar{\nu}_\ell$ decays is based on the Heavy Quark Expansion and leads to a predicted total decay rate with uncertainties below 5% [73, 100]. However, the total decay rate is hard to measure due to the large background from CKM-favored $\bar{B} \to X_c \ell \bar{\nu}_\ell$ transitions, and hence the theoretical methods differ from the $\bar{B} \to X_c \ell \bar{\nu}_\ell$ case. For a calculation of the partial decay rate in regions of phase space where $\bar{B} \to X_c \ell \bar{\nu}_\ell$ decays are suppressed one cannot use the HQE as for $b \to c$, rather the one needs to introduce non-perturbative distribution functions, the "shape functions" (SF) [101, 102]. Their exact from is not known, but its moments can be related to the HQE parameters known e.g from the $b \to c$ case.

The shape functions become important when the light-cone momentum component $P_+ \equiv E_X - |P_X|$ is not large compared to $\Lambda_{QCD}$, as is the case near the endpoint of the $\bar{B} \to X_u \ell \bar{\nu}_\ell$ lepton spectrum. Partial rates for $\bar{B} \to X_u \ell \bar{\nu}_\ell$ are predicted and measured in a variety of kinematic regions that differ in their sensitivity to shape-function effects.

At leading order in $1/m_b$ only a single shape function (SF) appears, which is universal for all heavy-to-light transitions [101, 102] and can be extracted in $\bar{B} \to X_s \gamma$ decays. At subleading order in $1/m_b$, several shape functions appear [103], along with "resolved photon contributions" specific for $\bar{B} \to X_s \gamma$ [104, 105], and thus the prescriptions that relate directly the partial rates for $\bar{B} \to X_s \gamma$ and $\bar{B} \to X_u \ell \bar{\nu}_\ell$ decays [106–114] are limited to leading order in $1/m_b$.

Existing approaches use parametrizations of the leading SF that respect constraints on the normalization and on the first and second moments, which are given in terms of the HQE parameters $\overline{\Lambda} = M_B - m_b$ and $\mu_\pi^2$, respectively. The relations between SF moments and the HQE parameters are known to second order in $\alpha_s$ [115]; as a result, measurements of HQE parameters from global fits to $\bar{B} \to X_c \ell \bar{\nu}_\ell$ and $\bar{B} \to X_s \gamma$ moments can be used to constrain the SF moments, as well as to provide accurate values of $m_b$ and other parameters for use in determining $|V_{ub}|$. Flexible parametrizations of the SF using orthogonal basis functions [116] or artificial neural networks [117] would allow global fits to inclusive $B$ meson decay data that incorporate the known short-distance contributions and renormalization properties of the SF.

HFLAV performs fits on the basis of several approaches, with varying degrees of model dependence. We will consider here the approaches documented in Ref. [118] (BLNP), Ref. [119] (GGOU) and Ref. [120] (DGE).

The triple differential rate in the variables

$$P_\ell = M_B - 2E_\ell, \quad P_- = E_X + |\vec{P}_X|, \quad P_+ = E_X - |\vec{P}_X| \tag{75.36}$$

is

$$\frac{d^3\Gamma}{dP_+\,dP_-\,dP_\ell} = \frac{G_F^2|V_{ub}|^2}{16\pi^2}(M_B - P_+) \Big\{(P_- - P_\ell)(M_B - P_- + P_\ell - P_+)\mathcal{F}_1 + (M_B - P_-)(P_- - P_+)\mathcal{F}_2 + (P_- - P_\ell)(P_\ell - P_+)\mathcal{F}_3\Big\}. \tag{75.37}$$

The "structure functions", $\mathcal{F}_i$, can be calculated using factorization theorems that have been proven to subleading order in the $1/m_b$ expansion [121].

The BLNP [118] calculation uses these factorization theorems to write the $\mathcal{F}_i$ terms as functions of perturbatively calculable hard coefficients $H$ and jet functions $J$, which are convolved with the (soft) light-cone distribution functions $S$, which is the shape functions of the $B$ meson. The calculation of $\mathcal{O}(\alpha_s^2)$ contributions [122, 123] is not yet complete and is not included in the $|V_{ub}|$ determination given below.

The leading order term in the $1/m_b$ expansion of the $\mathcal{F}_i$ terms contains a single non-perturbative function and is calculated to subleading order in $\alpha_s$, while at subleading order in the $1/m_b$ expansion there are several independent non-perturbative functions that have been calculated only at tree level in the $\alpha_s$ expansion.

A distinct approach (GGOU) [119] uses a hard, Wilsonian cut-off that matches the definition of the kinetic mass. The non-perturbative input is similar to what is used in BLNP, but the shape functions are defined differently. In particular, they are defined at finite $m_b$ and depend on the light-cone component $k_+$ of the $b$ quark momentum and on the momentum transfer $q^2$ to the leptons. These functions include subleading effects to all orders; as a result they are non-universal, with one shape function corresponding to each structure function in Eq. (75.37). Their $k_+$ moments can be computed in the OPE and related to observables and to the shape functions defined in Ref. [118].

Going to subleading order in $\alpha_s$ requires the definition of a renormalization scheme for the HQE parameters and for the SF. The relation between the moments of the SF and the forward matrix elements of local operators appearing the HQE is plagued by ultraviolet problems and requires additional renormalization. A scheme for improving this behavior was suggested in Ref. [118] and Ref. [124], which introduce a definition of the quark mass (the so-called shape-function scheme) based on the first moment of the measured $\bar{B} \to X_s\gamma$ photon energy spectrum. Likewise, the HQE parameters can be defined from measured moments of spectra, corresponding to moments of the SF.

There are various ideas to model the SF, but this requires additional assumptions. One approach (DGE) is the so-called "dressed gluon exponentiation" [120], where the perturbative result is continued into the infrared regime using the renormalon structure obtained in the large $\beta_0$ limit, where $\beta_0$ has been defined following Eq. (75.23). Other approaches make even stronger assumptions, such as in Ref. [125], which assumes an analytic behavior for the strong coupling in the infrared to perform an extrapolation of perturbation theory.

In order to reduce sensitivity to SF uncertainties, measurements that use a combination of cuts on the leptonic momentum transfer $q^2$ and the hadronic invariant mass $m_X$, as suggested in Ref. [126, 127], have been made. In general, efforts to extend the experimental measurements of $\bar{B} \to X_u\ell\bar{\nu}_\ell$ into charm-dominated regions (in order to reduce SF uncertainties) lead to an increased experimental sensitivity to the modeling of $\bar{B} \to X_u\ell\bar{\nu}_\ell$ decays, resulting in measured partial rates with an undesirable level of model dependence. The measurements quoted below have used a variety of functional forms to parametrize the leading SF; a specific error budget for one determination is quoted in the next section. In no case is the parametrization uncertainty estimated to be more than a 2% on $|V_{ub}|$.

Weak Annihilation [119,128,129] (WA) can in principle contribute significantly in the high-$q^2$ region of $\bar{B} \to X_u \ell \bar{\nu}_\ell$ decays. Estimates based on semileptonic $D_s$ decays [65,126,127,129] lead to a $\sim 2\%$ uncertainty on the total $\bar{B} \to X_u \ell \bar{\nu}_\ell$ rate from the $\Upsilon(4S)$. The $q^2$ spectrum of the WA contribution is not well known, but from the OPE it is expected to contribute predominantly at high $q^2$. More recent theoretical investigations [65,130,131] and a direct search [132] indicate that WA is a small effect, but may become a significant source of uncertainty for $|V_{ub}|$ measurements that accept only a small fraction of the full $\bar{B} \to X_u \ell \bar{\nu}_\ell$ phase space.

### 75.3.2 *Measurements*

We summarize the measurements used in the determination of $|V_{ub}|$ below. Given the improved precision and more rigorous theoretical interpretation of more recent measurements, determinations [133–136] done with LEP data are not considered in this review.

Inclusive electron momentum measurements [137–139] reconstruct a single charged electron to determine a partial decay rate for $\bar{B} \to X_u \ell \bar{\nu}_\ell$ near the kinematic endpoint. This results in a selection efficiency of order 50% and only modest sensitivity to the modeling of detector response. The inclusive electron momentum spectrum from $B\bar{B}$ events, after subtraction of the $e^+e^- \to q\bar{q}$ continuum background, is fitted to a model $\bar{B} \to X_u \ell \bar{\nu}_\ell$ spectrum and several components ($D\ell\bar{\nu}_\ell$, $D^*\ell\bar{\nu}_\ell$, ...) of the $\bar{B} \to X_c \ell \bar{\nu}_\ell$ background; the dominant uncertainties are related to this subtraction and modelling. The decay rate can be cleanly extracted for $E_e > 2.3\,\text{GeV}$, but this is deep in the SF region, where theoretical uncertainties are large. More recent measurements have increased the accessed phase phase. The resulting $|V_{ub}|$ values for various $E_e$ cuts are given in Table 75.1.

The most recent measurement [140] from BABAR is based on the inclusive electron spectrum and determines the partial branching fraction and $|V_{ub}|$ for $E_e > 0.8\,\text{GeV}$. The analysis shows that the partial branching fraction measurements can have signal model dependence when the kinematic acceptance includes regions dominated by $\bar{B} \to X_c \ell \bar{\nu}_\ell$ background. The model dependence enters primarily through the partial branching fractions, and arises because the signal yield fit has sensitivity to $\bar{B} \to X_u \ell \bar{\nu}_\ell$ decays only in regions with good signal to noise.

An untagged "neutrino reconstruction" measurement [141] from BABAR uses a combination [142] of a high-energy electron with a measurement of the missing momentum vector. This allows $\text{S/B} \sim 0.7$ for $E_e > 2.0\,\text{GeV}$ and a $\approx 5\%$ selection efficiency, but at the cost of a smaller accepted phase space for $\bar{B} \to X_u \ell \bar{\nu}_\ell$ decays and uncertainties associated with the determination of the missing momentum. The corresponding values for $|V_{ub}|$ are given in Table 75.1.

The large samples accumulated at the $B$ factories allow studies in which one $B$ meson is fully reconstructed and the recoiling $B$ decays semileptonically [143–146]. The experiments can fully reconstruct a "tag" $B$ candidate in about 0.5% (0.3%) of $B^+B^-$ ($B^0\bar{B}^0$) events. An electron or muon with center-of-mass momentum above 1.0 GeV is required amongst the charged tracks not assigned to the tag $B$ and the remaining particles are assigned to the $X_u$ system. The full set of kinematic properties ($E_\ell$, $m_X$, $q^2$, *etc.*) are available for studying the semileptonically decaying $B$, making possible selections that accept up to 90% of the full $\bar{B} \to X_u \ell \bar{\nu}_\ell$ rate; however, the sensitivity to $\bar{B} \to X_u \ell \bar{\nu}_\ell$ decays is still driven by the regions where $\bar{B} \to X_c \ell \bar{\nu}_\ell$ decays are suppressed. Despite requirements (e.g. on the square of the missing mass) aimed at rejecting events with additional missing particles, undetected or mis-measured particles from $\bar{B} \to X_c \ell \bar{\nu}_\ell$ decay (e.g., $K_L^0$ and additional neutrinos) remain an important source of uncertainty.

BABAR [143] and Belle [144,145] have measured partial rates with cuts on $m_X$, $m_X$ and $q^2$, $P_+$ and $E_\ell$ using the recoil method. In each case the experimental systematics have significant contributions from the modeling of $\bar{B} \to X_u \ell \bar{\nu}_\ell$ and $\bar{B} \to X_c \ell \bar{\nu}_\ell$ decays and from the detector response to charged particles, photons and neutral hadrons. The corresponding $|V_{ub}|$ values are given in Table 75.1.

### 75.3.3 $|V_{ub}|$ from inclusive partial rates

The measured partial rates and theoretical calculations from BLNP, GGOU and DGE described previously are used to determine $|V_{ub}|$ from all measured partial $\bar{B} \to X_u \ell \bar{\nu}_\ell$ rates [5]; selected values are given in Table 75.1. The correlations amongst the multiple BABAR recoil-based measurements [143] are fully accounted for in the average. The statistical correlations amongst the other measurements used in the average are small (due to small overlaps among signal events and large differences in S/B ratios) and have been ignored. Correlated systematic and theoretical errors are taken into account, both within an experiment and between experiments. As an illustration of the relative sizes of the uncertainties entering $|V_{ub}|$ we give the error breakdown for the GGOU average: statistical—1.6%; experimental—1.6%; $\bar{B} \to X_c \ell \bar{\nu}_\ell$ modeling—0.9%; $\bar{B} \to X_u \ell \bar{\nu}_\ell$ modeling—1.5%; HQE parameters ($m_b$) —1.9%; higher-order corrections—1.5%; $q^2$ modeling—1.3%; Weak Annihilation—$^{+0.0}_{-1.1}$%; SF parametrization—0.1%.

The averages quoted here are based on the following $m_b$ values: $m_b^{SF} = 4.582 \pm 0.023 \pm 0.018$ GeV for BLNP, $m_b^{\rm kin} = 4.554 \pm 0.018$ GeV for GGOU, and $m_b^{\overline{MS}} = 4.188 \pm 0.043$ GeV for DGE. The $m_b^{\rm kin}$ value is determined in a global fit to moments in the kinetic scheme; this value is translated into $m_b^{SF}$ and $m_b^{\overline{MS}}$ at fixed order in $\alpha_s$. The second uncertainty quoted on $m_b$ arises from the scheme translation.

**Table 75.1:** $|V_{ub}|$ (in units of $10^{-5}$) from inclusive $\bar{B} \to X_u \ell \bar{\nu}_\ell$ measurements. The first uncertainty on $|V_{ub}|$ is experimental, while the second includes both theoretical and HQE parameter uncertainties. The values are generally listed in order of increasing kinematic acceptance, $f_u$ (0.19 to 0.90), except for the BABAR $E_e$ >0.8 GeV measurement; those below the horizontal bar are based on recoil methods.

| Ref. | cut (GeV) | BLNP | GGOU | DGE |
|---|---|---|---|---|
| CLEO [137] | $E_e > 2.1$ | $422 \pm 49 \,^{+\,29}_{-\,34}$ | $423 \pm 49 \,^{+\,22}_{-\,31}$ | $386 \pm 45 \,^{+\,25}_{-\,27}$ |
| BABAR [141] | $E_e - q^2$ | $471 \pm 32 \,^{+\,33}_{-\,38}$ | not available | $435 \pm 29 \,^{+\,28}_{-\,30}$ |
| BABAR [139] | $E_e > 2.0$ | $452 \pm 26 \,^{+\,26}_{-\,30}$ | $452 \pm 26 \,^{+\,17}_{-\,24}$ | $430 \pm 24 \,^{+\,23}_{-\,25}$ |
| Belle [138] | $E_e > 1.9$ | $493 \pm 46 \,^{+\,26}_{-\,29}$ | $495 \pm 46 \,^{+\,16}_{-\,21}$ | $482 \pm 45 \,^{+\,23}_{-\,23}$ |
| BABAR [140] | $E_e > 0.8$ | $441 \pm 12 \,^{+\,27}_{-\,27}$ | $396 \pm 10 \,^{+\,17}_{-\,17}$ | $385 \pm 11 \,^{+\,8}_{-\,7}$ |
| BABAR [143] | $^{q^2>8}_{m_X<1.7}$ | $432 \pm 23 \,^{+\,26}_{-\,28}$ | $433 \pm 23 \,^{+\,24}_{-\,27}$ | $424 \pm 22 \,^{+\,18}_{-\,21}$ |
| BABAR [143] | $P_+ < 0.66$ | $409 \pm 25 \,^{+\,25}_{-\,25}$ | $425 \pm 26 \,^{+\,26}_{-\,27}$ | $417 \pm 25 \,^{+\,28}_{-\,37}$ |
| BABAR [143] | $m_X < 1.7$ | $403 \pm 22 \,^{+\,22}_{-\,22}$ | $410 \pm 23 \,^{+\,16}_{-\,17}$ | $422 \pm 23 \,^{+\,21}_{-\,27}$ |
| BABAR [143] | $E_\ell > 1$ | $433 \pm 24 \,^{+\,19}_{-\,21}$ | $444 \pm 24 \,^{+\,9}_{-\,10}$ | $445 \pm 24 \,^{+\,12}_{-\,13}$ |
| Belle [145] | $E_\ell > 1$ | $450 \pm 27 \,^{+\,20}_{-\,22}$ | $462 \pm 28 \,^{+\,9}_{-\,10}$ | $462 \pm 28 \,^{+\,13}_{-\,13}$ |
| HFLAV [5] | Combination | $444^{+\,13+\,21}_{-\,14-\,22}$ | $432 \pm 12 \,^{+\,12}_{-\,13}$ | $399 \pm 10 \,^{+\,9}_{-\,10}$ |

Hadronization uncertainties also impact the $|V_{ub}|$ determination. The theoretical expressions are valid at the parton level and do not incorporate any resonant structure (*e.g.* $\bar{B} \to \pi \ell \bar{\nu}_\ell$); this must be added to the simulated $\bar{B} \to X_u \ell \bar{\nu}_\ell$ event samples, since the detailed final state multiplicity and structure impacts the estimates of experimental acceptance and efficiency. The experiments have adopted procedures to input resonant structure while preserving the appropriate behavior in the kinematic variables ($q^2, E_\ell, m_X$) averaged over the sample, but these prescriptions are *ad hoc* and ultimately require *in situ* calibration. The resulting uncertainties have been estimated to be $\sim$ 1-2% on $|V_{ub}|$.

All calculations yield compatible $|V_{ub}|$ values and similar error estimates. The arithmetic mean

of the values and errors is $|V_{ub}| = (4.25 \pm 0.12_{\rm exp}\ ^{+0.15}_{-0.14\ \rm theo}) \times 10^{-3}$, although there is a spread of approximately 10% in the evaluations with the three theoretical models. For reasons discussed below, we assign an additional uncertainty due to model dependence that is not reflected in the HFLAV averages. As highlighted in the BABAR analysis [140], model dependence entering measurement procedures can be sizeable, and is not consistently treated across analyses. Many of the analyses shown in Table 75.1 were based on partial branching fraction measurements determined in a single model (i.e. the one used by that analysis when simulating $\bar{B} \to X_u \ell \bar{\nu}_\ell$ decays), although in some cases simulated events were weighted to match the expected spectra in other models and the differences introduced as systematic uncertainties, e.g. Ref. [145]. The $|V_{ub}|$ value quoted by HFLAV for each model are, typically, derived from this unique partial branching fraction combined with another model-specific partial rate calculation. This translation from a single partial branching fraction into $|V_{ub}|$ values in different models suffers, in principle, from the difficulties made explicit in the recent BABAR measurement. The model dependence in the partial branching fraction is sensitive to how the model predictions compare in the restricted region with good signal-to-noise, not by how they compare when integrated over the full kinematic range used in the fit. This effect needs to be accounted for by the experiments; the published results are insufficient to determine it. To account for the range in results using the different theoretical models, we take half of the spread of the averages as an additional systematic uncertainty, denoted $\Delta$BF. With this addition, the inclusive $|V_{ub}|$ average is

$$|V_{ub}| = (4.25 \pm 0.12_{\rm exp}\ ^{+0.15}_{-0.14\ \rm theo} \pm 0.23_{\Delta \rm BF}) \times 10^{-3} \quad \text{(inclusive)}. \tag{75.38}$$

### 75.3.4 $|V_{ub}|$ *from exclusive decays*

Exclusive charmless semileptonic decays offer a complementary means of determining $|V_{ub}|$. For the experiments, the specification of the final state provides better background rejection, but the branching fraction to a specific final state is typically only a few percent of that for inclusive decays. For theory, the calculation of the form factors for $\bar{B} \to X_u \ell \bar{\nu}_\ell$ decays is challenging, but brings in a different set of uncertainties from those encountered in inclusive decays. In this review we focus on $\bar{B} \to \pi \ell \bar{\nu}_\ell$, as it is the most promising decay mode for both experiment and theory. Measurements of other exclusive $\bar{B} \to X_u \ell \bar{\nu}_\ell$ decays can be found in Refs. [147–160].

### 75.3.5 $\bar{B} \to \pi \ell \bar{\nu}_\ell$ *form factor calculations*

The relevant form factors for the decay $\bar{B} \to \pi \ell \bar{\nu}_\ell$ are usually defined as

$$\langle \pi(p_\pi) | V^\mu | B(p_B) \rangle = f_+(q^2) \left[ p_B^\mu + p_\pi^\mu - \frac{m_B^2 - m_\pi^2}{q^2} q^\mu \right] + f_0(q^2) \frac{m_B^2 - m_\pi^2}{q^2} q^\mu \tag{75.39}$$

in terms of which the rate becomes (in the limit $m_\ell \to 0$)

$$\frac{d\Gamma}{dq^2} = \frac{G_F^2 |V_{ub}|^2}{24\pi^3} |p_\pi|^3 |f_+(q^2)|^2, \tag{75.40}$$

where $p_\pi$ is the pion momentum in the $B$ meson rest frame.

Currently available non-perturbative methods for the calculation of the form factors include lattice QCD (LQCD) and light-cone sum rules (LCSR). The two methods are complementary in phase space, since the lattice calculation is restricted to the kinematical range of high momentum transfer, $q^2$, to the leptons, while light-cone sum rules provide information near $q^2 = 0$. Interpolations between these two regions can be constrained by unitarity and analyticity.

Lattice simulations for $B \to \pi \ell \bar{\nu}$ and $B_s \to K \ell \bar{\nu}$ transitions, where quark loop effects are fully incorporated, have been performed by the Fermilab/MILC [161, 162], HPQCD [163, 164] and

RBC/UKQCD [165] collaborations. The calculations differ in the way the $b$ quark is simulated. While HPQCD is using nonrelativistic QCD, Fermilab/MILC and RBC/UKQCD are using relativistic $b$ quarks with the Fermilab and Columbia heavy-quark forumulations. The results agree within the quoted errors. The form factor $f_+$ evaluated at $q^2 = 20\,\mathrm{GeV}^2$ has an estimated uncertainty of 3.4%, where the leading contribution is due to the chiral-continuum extrapolation fit, which includes statistical and heavy-quark discretization errors. However, the lattice simulations are restricted to the region of large $q^2$, i.e. the region $q^2_{\rm max} > q^2 \gtrsim 15\,\mathrm{GeV}^2$.

The extrapolation to small values of $q^2$ is performed using guidance from analyticity and unitarity. Making use of the heavy-quark limit, stringent constraints on the shape of the form factor can be derived [166], and the conformal mapping of the kinematical variables onto the complex unit disc yields a rapidly converging series in the variable

$$z = \frac{\sqrt{t_+ - t_-} - \sqrt{t_+ - q^2}}{\sqrt{t_+ - t_-} + \sqrt{t_+ - q^2}}\,, \tag{75.41}$$

where $t_\pm = (M_B \pm m_\pi)^2$. The use of lattice data in combination with experimental measurements of the differential decay rate provides a stringent constraint on the shape of the form factor in addition to precise determination of $|V_{ub}|$ [167].

Another established non-perturbative approach to obtain the form factors is through Light-Cone QCD Sum Rules (LCSR), which, however, are not at the same footing as LQCD. LCSR provide an estimate for the product $f_B f_+(q^2)$, valid in the region $0 < q^2 \lesssim 12$ GeV. The determination of $f_+(q^2)$ itself requires knowledge of the decay constant $f_B$, which is usually obtained by replacing $f_B$ by its two-point QCD (SVZ) sum rule [168] in terms of perturbative and condensate contributions. The advantage of this procedure is the approximate cancellation of various theoretical uncertainties in the ratio $(f_B f_+)/(f_B)$.

The LCSR for $f_B f_+$ is based on the light-cone OPE of the relevant vacuum-to-pion correlation function, calculated in full QCD at finite $b$-quark mass. The resulting expressions comprise a triple expansion: in the twist $t$ of the operators near the light-cone, in $\alpha_s$, and in the deviation of the pion distribution amplitudes from their asymptotic form, which is fixed from conformal symmetry. The state-of-the-art calculations include the leading twists two, three and four with full one-loop $\alpha_s$ corrections [169, 170] and partial two-loop corrections [171]. Higher-twist contributions have been investigated in Ref. [172], which turn out to be small. Nevertheless, estimates based on LCSR are always affected by an systematic uncertainty, which is hard to quantify.

A detailed statistical analysis including the various correlations has been performed in Ref. [173], also including unitarity bounds on the form factor. The results obtained are fully compatible with the lattice QCD calculations of the form factor. For a determination of $V_{ub}$ one may use the partial rate expressed by the integral

$$\begin{aligned} \Delta\zeta(0, q^2_{max}) &= \frac{G_F^2}{24\pi^3} \int_0^{q^2_{max}} dq^2\, p_\pi^3 |f_+(q^2)|^2 \\ &= \frac{1}{|V_{ub}|^2 \tau_{B_0}} \int_0^{q^2_{max}} dq^2\, \frac{d\mathcal{B}(B \to \pi \ell \nu)}{dq^2}\,, \end{aligned} \tag{75.42}$$

for which the light-cone sum rule gives [173]

$$\Delta\zeta(0, 12\,\mathrm{GeV}^2) = 5.25^{+0.68}_{-0.54}\,\mathrm{ps}^{-1}. \tag{75.43}$$

The uncertainty in this integral is about ten percent, which translates to a theoretical uncertainty of about five percent for the determination of $V_{ub}$ with this method.

### 75.3.6 $\bar{B} \to \pi\ell\bar{\nu}_\ell$ measurements

The $\bar{B} \to \pi\ell\bar{\nu}_\ell$ measurements fall into two broad classes: untagged, in which case the reconstruction of the missing momentum of the event serves as an estimator for the unseen neutrino, and tagged, in which the second $B$ meson in the event is fully reconstructed in either a hadronic or semileptonic decay mode. The tagged measurements have better $q^2$ resolution, high and uniform acceptance and S/B as high as 10, but lower statistical power. The untagged measurements have somewhat higher background (S/B $< 1$) and make slightly more restrictive kinematic cuts, but still provide statistical power precision on the $q^2$ dependence of the form factor.

CLEO has analyzed $\bar{B} \to \pi\ell\bar{\nu}_\ell$ and $\bar{B} \to \rho\ell\bar{\nu}_\ell$ using an untagged analysis [154–156]. Similar analyses have been done at BABAR [157–160] and Belle [174]. The leading systematic uncertainties in the untagged $\bar{B} \to \pi\ell\bar{\nu}_\ell$ analyses are associated with modeling the missing momentum reconstruction, with background from $\bar{B} \to X_u\ell\bar{\nu}_\ell$ decays and $e^+e^- \to q\bar{q}$ continuum events, and with varying the form factor used to model $\bar{B} \to \rho\ell\bar{\nu}_\ell$ decays.

Analyses [149, 175] based on reconstructing a $B$ in the $\bar{D}^{(*)}\ell^+\nu_\ell$ decay mode and looking for a $\bar{B} \to \pi\ell\bar{\nu}_\ell$ or $\bar{B} \to \rho\ell\bar{\nu}_\ell$ decay amongst the remaining particles in the event make use of the fact that the $B$ and $\bar{B}$ are back-to-back in the $\Upsilon(4S)$ frame to construct a discriminant variable that provides a signal-to-noise ratio above unity for all $q^2$ bins. A related technique was discussed in Ref. [176]. BABAR [175] and Belle [147] have also used their samples of $B$ mesons reconstructed in hadronic decay modes to measure exclusive charmless semileptonic decays, resulting in very clean but smaller samples. The dominant systematic uncertainties in the tagged analyses arise from tag calibration.

$|V_{ub}|$ can be obtained from the average $\bar{B} \to \pi\ell\bar{\nu}_\ell$ branching fraction and the measured $q^2$ spectrum. Fits to the $q^2$ spectrum using a theoretically motivated parametrization (e.g. "BCL" from Ref. [44]) remove most of the model dependence from theoretical uncertainties in the shape of the spectrum. The most sensitive method for determining $|V_{ub}|$ from $\bar{B} \to \pi\ell\bar{\nu}_\ell$ decays employs a simultaneous fit [5, 161, 166, 167, 177, 178] to measured experimental partial rates and lattice points versus $q^2$ (or $z$) to determine $|V_{ub}|$ and the first few coefficients of the expansion of the form factor in $z$. We quote the result from Ref. [5], which uses as experimental input an average of the measurements in Refs. [147, 157, 160, 174] and an average [179] of the LQCD input from Ref. [161] and Ref. [165]. The probability of the $q^2$ measurement average is 6%. The average for the total $B^0 \to \pi^-\ell^+\nu_\ell$ branching fraction is obtained by summing up the partial branching fractions:

$$\mathcal{B}(B^0 \to \pi^-\ell^+\nu_\ell) = (1.50 \pm 0.02_{\rm stat} \pm 0.06_{\rm syst}) \times 10^{-4} \tag{75.44}$$

The corresponding value of $|V_{ub}|$ with this approach is found to be

$$|V_{ub}| = (3.70 \pm 0.10 \pm 0.12\,) \times 10^{-3} \quad \text{(exclusive)}, \tag{75.45}$$

where the first uncertainty is experimental and the second is from theory. Adding an additional constraint using input [171] from LCSR gives [5] $|V_{ub}| = (3.67 \pm 0.09 \pm 0.12\,) \times 10^{-3}$ (exclusive, LQCD+LCSR). Consistent results for $|V_{ub}|$ were found in a fit reported in Ref. [25].

## 75.4 Semileptonic $b$-baryon decays and determination of $|V_{ub}|/|V_{cb}|$

*Summary:* A significant sample of $\Lambda_b^0$ baryons is available at the LHCb experiment, and methods have been developed to study their semileptonic decays. Both $\Lambda_b^0 \to p\mu\bar{\nu}$ and $\Lambda_b^0 \to \Lambda_c^+\mu\bar{\nu}$ decays have been measured at LHCb, and the ratio of branching fractions to these two decay modes is used to determine the ratio $|V_{ub}/V_{cb}|$. Averaging the LHCb determination with those obtained from inclusive and exclusive $B$ meson decays, we find

$$|V_{ub}|/|V_{cb}| = 0.092 \pm 0.008 \quad \text{(average)} \tag{75.46}$$

where the average has $p(\chi^2) = 0.9\%$ and the uncertainty has been scaled by a factor $\sqrt{\chi^2/2} = 2.2$. In light of the poor consistency of the three determinations considered, the average should be treated with caution.

### 75.4.1 $\Lambda_b^0 \to \Lambda_c^+ \mu\bar{\nu}$ and $\Lambda_b^0 \to p\mu\bar{\nu}$

The $\Lambda_b^0 \to \Lambda_c^+$ and $\Lambda_b^0 \to p$ semileptonic transitions are described in terms of six form factors each. The three form factors corresponding to the vector current can be defined as [180]

$$\begin{aligned}\langle F(p',s')|\bar{q}\,\gamma_\mu\, b|\Lambda_b^0(p,s)\rangle = \bar{u}_F(p',s')\Bigg\{ & f_0(q^2)\,(M_{\Lambda_b^0} - m_F)\,\frac{q_\mu}{q^2} \\ & + f_+(q^2)\,\frac{M_{\Lambda_b^0}+m_F}{s_+}\left(p_\mu + p'_\mu - \frac{q_\mu}{q^2}\,(M^2_{\Lambda_b^0} - m_F^2)\right) \\ & + f_\perp(q^2)\left(\gamma_\mu - \frac{2m_F}{s_+}\,p_\mu - \frac{2M_{\Lambda_b^0}}{s_+}\,p'_\mu\right)\Bigg\}\, u_{\Lambda_b^0}(p,s)\,, \end{aligned} \tag{75.47}$$

where $F = p$ or $\Lambda_c^+$ and where we define $s_\pm = (M_{\Lambda_b^0} \pm m_F)^2 - q^2$. At vanishing momentum transfer, $q^2 \to 0$, the kinematic constraint $f_0(0) = f_+(0)$ holds. The form factors are defined in such a way that they correspond to time-like (scalar), longitudinal and transverse polarization with respect to the momentum-transfer $q^\mu$ for $f_0$, $f_+$ and $f_\perp$, respectively. Furthermore we have chosen the normalization in such a way that for $f_0, f_+, f_\perp \to 1$ one recovers the expression for point-like baryons.

Likewise, the expression for the axial-vector current is

$$\begin{aligned}\langle F(p',s')|\bar{q}\,\gamma_\mu\gamma_5\, b|\Lambda_b^0(p,s)\rangle = & -\bar{u}_F(p',s')\gamma_5 \\ & \Bigg\{ g_0(q^2)\,(M_{\Lambda_b^0} + m_F)\,\frac{q_\mu}{q^2} \\ & + g_+(q^2)\,\frac{M_{\Lambda_b^0}-m_F}{s_-}\left(p_\mu + p'_\mu - \frac{q_\mu}{q^2}\,(M^2_{\Lambda_b^0} - m_F^2)\right) \\ & + g_\perp(q^2)\left(\gamma_\mu + \frac{2m_F}{s_-}\,p_\mu - \frac{2M_{\Lambda_b^0}}{s_-}\,p'_\mu\right)\Bigg\}\, u_{\Lambda_b^0}(p,s)\,, \end{aligned} \tag{75.48}$$

with the kinematic constraint $g_0(0) = g_+(0)$ at $q^2 \to 0$.

The form factors have been discussed in the heavy quark limit; assuming both $b$ and $c$ as heavy, all the form factors $f_i$ and $g_i$ for the case $\Lambda_b^0 \to \Lambda_c^+ \mu\nu$ turn out to be identical [180]

$$f_0 = f_+ = f_\perp = g_0 = g_+ = g_\perp = \xi_B \tag{75.49}$$

and equal to the Isgur Wise function $\xi_B$ for baryons. In the limit of a light baryon in the final state, the number of independent form factors is still reduced to two through the heavy quark symmetries of the $\Lambda_b^0$. It should be noted that the $\Lambda_b^0 \to (p/\Lambda_c^+)\mu\nu$ decay rates peak at high $q^2$, which facilitates both lattice QCD calculations and experimental measurements.

The form factors for $\Lambda_b^0$ decays have been studied with lattice QCD [181]. Based on these results the differential rates for both $\Lambda_b^0 \to \Lambda_c^+ \mu\bar{\nu}$ as well as for $\Lambda_b^0 \to p\mu\bar{\nu}$ can be predicted in the full phase space. In particular, for the experimentally interesting region they find the ratio of decay rates to be [181]

$$\frac{\mathcal{B}(\Lambda_b^0 \to p\mu\bar{\nu})_{q^2>15\,\mathrm{GeV}^2}}{\mathcal{B}(\Lambda_b^0 \to \Lambda_c^+\mu\bar{\nu})_{q^2>7\,\mathrm{GeV}^2}} = (1.471 \pm 0.095 \pm 0.109)\left|\frac{V_{ub}}{V_{cb}}\right|^2 \tag{75.50}$$

where the first uncertainty is statistical and the second, systematic.

### 75.4.2 *Measurements at LHCb*

The LHCb experiment has measured the branching fractions of the semileptonic decays $\Lambda_b^0 \to \Lambda_c^+ \mu\bar{\nu}$ and $\Lambda_b^0 \to p\mu\bar{\nu}$, from which they determine $|V_{ub}|/|V_{cb}|$. This is the first such determination at a hadron collider, the first to use a $b$ baryon decay, and the first observation of $\Lambda_b^0 \to p\mu\bar{\nu}$. Excellent vertex resolution allows the $p\mu$ and production vertices to be separated, which permits the calculation of the transverse momentum $p_\perp$ of the $p\mu$ pair relative to the $\Lambda_b^0$ flight direction. The corrected mass, $m_{\rm corr} = \sqrt{p_\perp^2 + m_{p\mu}^2} + p_\perp$, peaks at the $\Lambda_b^0$ mass for signal decays and provides good discrimination against background combinations. The topologically similar decay $\Lambda_b^0 \to \Lambda_c^+ \mu\bar{\nu}$ is also measured, which eliminates the need to know the production cross-section or absolute efficiencies. Using vertex and $\Lambda_b^0$ mass constraints, $q^2$ can be determined up to a two-fold ambiguity. The LHCb analysis requires both solutions to be in the high $q^2$ region to minimise contamination from the low $q^2$ region. Their result [182], rescaled [5] to take into account the recent branching fraction measurement [183] $\mathcal{B}(\Lambda_c^+ \to pK^-\pi^+) = (6.28 \pm 0.32)\%$, is

$$\frac{\mathcal{B}(\Lambda_b^0 \to p\mu\bar{\nu})_{q^2>15{\rm GeV}^2}}{\mathcal{B}(\Lambda_b^0 \to \Lambda_c^+ \mu\bar{\nu})_{q^2>7{\rm GeV}^2}} = (0.92 \pm 0.04 \pm 0.07) \times 10^{-2} \quad . \tag{75.51}$$

The largest systematic uncertainty is from the measured $\mathcal{B}(\Lambda_c^+ \to pK^-\pi^+)$; uncertainties due to trigger, tracking and the $\Lambda_c^+$ selection efficiency are each about 3%.

A recent LHCb analysis [184] measures the normalized $q^2$ spectrum and finds good agreement with the shape calculated with lattice QCD [181].

### 75.4.3 *The ratio $|V_{ub}|/|V_{cb}|$*

The ratio of matrix elements, $|V_{ub}|/|V_{cb}|$, is often required when testing the compatibility of a set of measurements with theoretical predictions. It can be determined from the ratio of branching fractions measured by the LHCb experiment, quoted in the previous section. It can also be calculated based on the $|V_{ub}|$ and $|V_{cb}|$ values quoted earlier in this review.

As previously noted, the decay rate for $\Lambda_b^0 \to p\mu\bar{\nu}$ peaks at high $q^2$ where the calculation of the associated form factors using lattice QCD is under good control. Using the measured ratio from Eq. (75.51) along with the calculations of Ref. [181] results in [5]

$$|V_{ub}|/|V_{cb}| = 0.079 \pm 0.004 \pm 0.004 \quad \text{(LHCb)}. \tag{75.52}$$

where the first uncertainty is experimental and the second is from the LQCD calculation.

Given the similarities in the theoretical frameworks used for charmed and charmless decays, we choose to quote the ratio $|V_{ub}|/|V_{cb}|$ separately for inclusive and exclusive $B$ decays, as discussed earlier:

$$|V_{ub}|/|V_{cb}| = 0.101 \pm 0.007 \quad \text{(inclusive)}, \tag{75.53}$$

$$|V_{ub}|/|V_{cb}| = 0.094 \pm 0.005 \quad \text{(exclusive)}. \tag{75.54}$$

The respective determinations of $|V_{ub}|$ and $|V_{cb}|$ are taken to be uncorrelated in the ratio, although there could be some small cancellations of the uncertainties in both the experimental the theoretical input. We average the mesonic decay values, along with the baryonic result in Eq. (75.52), weighting by relative errors. The average has $p(\chi^2) = 4\%$, so we scale the uncertainty by a factor $\sqrt{\chi^2/2} = 1.8$ to find

$$|V_{ub}|/|V_{cb}| = 0.091 \pm 0.006 \quad \text{(average)}. \tag{75.55}$$

## 75.5 Semitauonic decays

*Summary:* Semileptonic decays to third-generation leptons provide sensitivity to non-Standard Model amplitudes, such as from a charged Higgs boson [185–188] and from leptoquarks [189–195]. The ratios of branching fractions of semileptonic decays involving tau leptons to those involving $\ell = e/\mu$, $R(D^{(*)}) \equiv \mathcal{B}(\bar{B} \to D^{(*)}\tau\bar{\nu}_\tau)/\mathcal{B}(\bar{B} \to D^{(*)}\ell\bar{\nu}_\ell)$, are predicted with good precision in the Standard Model [42,43,47,196,197]. For $R(D)$ and $R(D^*)$ we use the values obtained in [198]

$$R(D)^{\rm SM} = 0.297 \pm 0.003 \ ,$$
$$R(D^*)^{\rm SM} = 0.252 \pm 0.003 \ . \tag{75.56}$$

Measurements [199–207] of these ratios yield higher values; averaging $B$-tagged measurements of $R(D)$ and $R(D^*)$ at the $\Upsilon(4S)$ and the LHCb measurements of $R(D^*)$ yields [208]

$$R(D)^{\rm meas} = 0.340 \pm 0.027 \pm 0.013 \ ,$$
$$R(D^*)^{\rm meas} = 0.295 \pm 0.011 \pm 0.008 \ , \tag{75.57}$$

with a linear correlation of $-0.38$. These values exceed Standard Model predictions by $1.4\sigma$ and $2.5\sigma$, respectively. A variety of new physics models have been proposed, see eg. [185–195] to explain this excess. Most models proposed to explain the semitauonic decay excesses tend to, but not always have very little impact on semileptonic decays involving muons or electrons, so they do not significantly modify the $|V_{ub}|$ or $|V_{cb}|$ determinations discussed previously in this review. Lepton flavour universality in the ratio of electron and muon modes has been confirmed in a direct ratio measurement, $\mathcal{B}(\bar{B} \to D^{(*)}e\bar{\nu}_e)/\mathcal{B}(\bar{B} \to D^{(*)}e\bar{\nu}_\mu) = 1.01 \pm 0.03$, from Belle [40]. The uncertainty is dominated by lepton identification uncertainties that do not cancel in the ratio.

### 75.5.1 *Sensitivity of $\bar{B} \to D^{(*)}\tau\bar{\nu}_\tau$ to additional amplitudes*

In addition to the helicity amplitudes present for decays to $e\bar{\nu}_e$ and $\mu\bar{\nu}_\mu$, decays proceeding through $\tau\bar{\nu}_\tau$ include a scalar amplitude $H_s$. The differential decay rate is given by [209]

$$\frac{d\Gamma}{dq^2} = \frac{G_F^2\,|V_{cb}|^2\,|\mathbf{p}^*_{D^{(*)}}|q^2}{96\pi^3 m_B^2}\left(1-\frac{m_\tau^2}{q^2}\right)^2$$
$$\left[(|H_+|^2+|H_-|^2+|H_0|^2)\left(1+\frac{m_\tau^2}{2q^2}\right)+\frac{3m_\tau^2}{2q^2}|H_s|^2\right], \tag{75.58}$$

where $|\mathbf{p}^*_{D^{(*)}}|$ is the 3-momentum of the $D^{(*)}$ in the $\bar{B}$ rest frame and the helicity amplitudes $H$ depend on the four-momentum transfer $q^2$. All four helicity amplitudes contribute to $\bar{B} \to D^*\tau\bar{\nu}_\tau$, while only $H_0$ and $H_s$ contribute to $\bar{B} \to D\tau\bar{\nu}_\tau$; as a result, new physics contributions can produce larger effects in the latter mode. Semi-leptonic $B$ decays into a $\tau$ lepton provide a stringent test of the two-Higgs doublet model of type II (2HDMII), i.e. where the two Higgs doublets couple separately to up- and down-type quarks. The distinct feature of the 2HDMII is that the contributions of the charged scalars scale as $m_\tau^2/m_{H^+}^2$, since the couplings to the charged Higgs particles are proportional to the mass of the lepton. As a consequence, one may expect visible effects in decays into a $\tau$, but only small effects for decays into $e$ and $\mu$. The present data rule out the 2HDMII, see below.

### 75.5.2 *Measurement of $R(D^{(*)})$*

$\bar{B} \to D^{(*)}\tau\bar{\nu}_\tau$ decays have been studied at the $\Upsilon(4S)$ resonance and in $pp$ collisions. At the $\Upsilon(4S)$, the majority of experimental measurements are based on signatures that consist of a $D$ or $D^*$ meson, an electron or muon (denoted here by $\ell$) from the decay $\tau \to \ell\nu_\tau\bar{\nu}_\ell$, a fully-reconstructed

decay of the second $B$ meson in the event, and multiple missing neutrinos. One analysis reconstructs the $\tau$ in a hadronic mode. The analyses that use hadronic $B$ tags separate signal decays from $\bar{B} \to D^{(*)}\ell\bar{\nu}_\ell$ decays using the lepton momentum and the measured missing mass squared; decays with only a single missing neutrino peak sharply at zero in this variable, while the signal is spread out to positive values. When a semileptonic $B$ tag is used, the discrimination between signal and $\bar{B} \to D^{(*)}\ell\bar{\nu}_\ell$ decays comes from the calorimeter energy that is unassociated with any particle used in the reconstruction of the $B$ meson candidates, the measured missing mass squared and the cosine of the angle between the $D^*\ell$ system and its parent $B$ meson, which is calculated under the assumption that only one particle (a neutrino) is missing. In both these approaches, background from $\bar{B} \to D^{**}\ell\bar{\nu}_\ell$ decays with one or more unreconstructed particles is challenging to separate from signal, as is background from $\bar{B} \to D^{(*)}H_{\bar{c}}X$ (where $H_{\bar{c}}$ is a hadron containing a $\bar{c}$ quark) decays. The leading sources of systematic uncertainty are due to the limited size of simulation samples used in constructing the PDFs, the composition of the $D^{**}$ states, efficiency corrections, and cross-feed (swapping soft particles between the signal and tag $B$).

The most recent measurement from Belle [205] uses semileptonic $B$ tags and leptonic $\tau$ decays to simultaneously measure $R(D^*)$ and $R(D)$. The measurement provides the single most precise determination of these ratios, combining results from charged and neutral $B$ decays, and is compatible with the standard model expectation within $1\sigma$.

In addition to the ratio measurements, the Belle experiment has recently performed polarization measurements of the $\tau$ [204] and $D^*$ [210] respectively. The $\tau$ polarization measurement uses hadronic $B$ tags and $\tau^-$ decays to $\pi^-\nu_\tau$ or $\rho^-\nu_\tau$. The main discriminant variables are the measured missing mass squared and the unassociated calorimeter energy. This measurement provides the first determination of the $\tau$ polarization in the $\bar{B} \to D^*\tau\bar{\nu}_\tau$ decay, $\mathcal{P}(D^*) = -0.38 \pm 0.51\ ^{+0.21}_{-0.16}$, compatible with the standard model expectation [20], $-0.476^{+0.037}_{-0.034}$.

The main uncertainties on the $R(D^*)$ measurement come from the composition of the hadronic $B$ background and from modeling of semileptonic $B$ decays and mis-reconstructed $D^*$ mesons. The $D^*$ polarization measurement uses an inclusive tag approach based on Refs. [211, 212], and reconstructs the $\tau$ decays in $\ell\nu_\tau\bar{\nu}_\ell$ and $\pi^+\bar{\nu}_\tau$ channels. The main discriminant variables are $X_{\rm miss}$, a quantity that approximates missing mass but does not depend on tag $B$ reconstruction, the visible energy of the event, and the beam-energy constrained mass, $M_{\rm bc}$, of the inclusively reconstructed tag side $B$. This measurement provides the first determination of the $D^*$ longitudinal polarization fraction in the $\bar{B} \to D^*\tau\bar{\nu}_\tau$ decay, $\mathcal{F}_\mathcal{L}(D^*) = -0.38 \pm 0.60\ ^{+0.08}_{-0.04}$, compatible with the standard model expectation [213] within $1.7\sigma$.

The LHCb experiment has studied the decay $\bar{B} \to D^{*+}\tau\bar{\nu}_\tau$ with $D^{*+} \to D^0\pi^+$, $D^0 \to K^-\pi^+$ and $\tau \to \mu\nu_\tau\bar{\nu}_\mu$ in $pp$ collisions. Their analysis [206] takes advantage of the measurable flight lengths of $b$ and $c$ hadrons and $\tau$ leptons. A multivariate discriminant is used to select decays where no additional charged particles are consistent with coming from the signal decay vertices. The separation between the primary and $B$ decay vertices is used to calculate the momentum of the $B$ decay products transverse to the $B$ flight direction. The longitudinal component of the $B$ momentum can be estimated based on the visible decay products; this allows a determination of the $B$ rest frame, with modest resolution, and enables the calculation of the same discrimination variables available at the $e^+e^-$ $B$ factories. The (rest frame) muon energy, missing mass-squared and $q^2$ are used in a 3-$d$ fit. The most recent LHCb result [214] on $R(D^*)$ uses three-prong $\tau$ decays that take advantage of their excellent vertex resolution to isolate the $\tau$ decay from hadronic background. A 3-$d$ fit is performed to determine the signal yield, based on the $\tau$-$\nu_\tau$ pair $q^2$, the $\tau$ lifetime, as well as a boosted decision tree classifier based on isolation, invariant mass and flight distance information. The leading sources of systematic uncertainty are due to the size of the simulation sample used in constructing the fit templates, uncertainties in modelling the background

from hadronic $\bar{B} \to D^{(*)} H_{\bar{c}} X$ decays, as well as reconstruction and trigger effects. The result is normalized to $B^0 \to D^{*-}\pi^+\pi^-\pi^+$ and found to be $1\sigma$ from the standard model expectation (using the expectation value quoted here). An analogous measurement of $B_c \to J/\psi\tau\bar{\nu}_\tau$ was performed by the LHCb measurement [215], in leptonic $\tau$ decays. The result, $R(J/\psi) = 0.71 \pm 0.17 \pm 0.18$, while relatively high is compatible within $2\sigma$ of the standard model. Systematic uncertainties are dominated by form factors, as $B_c$ decays are relatively unexplored.

Measurements from BABAR [199–201], Belle [202–205] and LHCb [206, 214] result in values for $R(D)$ and $R(D^*)$ that exceed Standard Model predictions. Table 75.2 lists these values and their average. The simultaneous measurements of $R(D)$ and $R(D^*)$ have linear correlation coefficients of $-0.27$ (BABAR [200, 201]), $-0.49$ (Belle hadronic tag [202]) and $-0.51$ (Belle semileptonic tag [205]); the $R(D)$ and $R(D^*)$ averages have a correlation of $-0.38$. Two early untagged Belle measurements [211, 212] are subject to larger systematic uncertainties, with a breakdown of the respective contributions that is inconsistent with the more recent determinations, hence they cannot be reliably combined in the average. All three experiments assume the Standard Model kinematic distributions for $\bar{B} \to D^{(*)}\tau\bar{\nu}_\tau$ in their determinations of the branching fraction ratios.

**Table 75.2:** Measurements of $R(D)$ and $R(D^*)$, their correlations, $\rho$, and the combined averages [208].

| | | $R(D) \times 10^2$ | $R(D^*) \times 10^2$ | $\rho$ |
|---|---|---|---|---|
| BABAR [200, 201] | $B^0$, $B^+$ | $44.0 \pm 5.8 \pm 4.2$ | $33.2 \pm 2.4 \pm 1.8$ | $-0.27$ |
| Belle [202] | $B^0$, $B^+$ | $37.5 \pm 6.4 \pm 2.6$ | $29.3 \pm 3.8 \pm 1.5$ | $-0.49$ |
| Belle [204, 216] | $B^0$, $B^+$ | | $27.0 \pm 3.5 \,^{+\,2.8}_{-\,2.5}$ | |
| Belle [205] | $B^0$, $B^+$ | $30.7 \pm 3.7 \pm 1.6$ | $28.3 \pm 1.8 \pm 1.4$ | $-0.51$ |
| LHCb [206] | $B^0$ | | $33.6 \pm 2.7 \pm 3.0$ | |
| LHCb [214] | $B^0$ | | $28.0 \pm 1.8 \pm 2.9$ | |
| Average | $B^0$, $B^+$ | $34.0 \pm 2.7 \pm 1.3$ | $29.5 \pm 1.1 \pm 0.8$ | $-0.38$ |

The measurement combination in the $R(D) - R(D^*)$ plane is shown in Fig. 75.1, compared with an arithetic average of predictions from Refs. [47, 217, 218]. The figure is taken from Ref. [5]. The tension between the SM prediction and the measurements is at the level of $1.4\sigma$ ($R(D)$) and $2.5\sigma$ ($R(D^*)$); if one considers these deviations together the significance rises to $3.1\sigma$. This motivates speculation on possible new physics contributions, although this discrepancy has reduced with respect to previous editions of the RPP due to the results reported in Refs. [205, 214, 216]. There is some tension in the combination coming from the BABAR measurement, the only measurement to claim a deviation from the SM of more than $3\sigma$, although the $p-$value of the full combination is an acceptable 27%.

The current discussion of $R(D)$ and $R(D^*)$ may be embedded in the theoretical analysis of the other anomalies that have been observed in semileptonic FCNC ($b \to s\ell\ell$) transitions. More sophisticated approaches fit the data to a general effective Hamiltonian. Matching this effective Hamiltonian to simplified models, the current situation of the anomalies seems to be compatible with scenarios with an additional $Z'$ or a leptoquark scenario, see eg. [189–195].

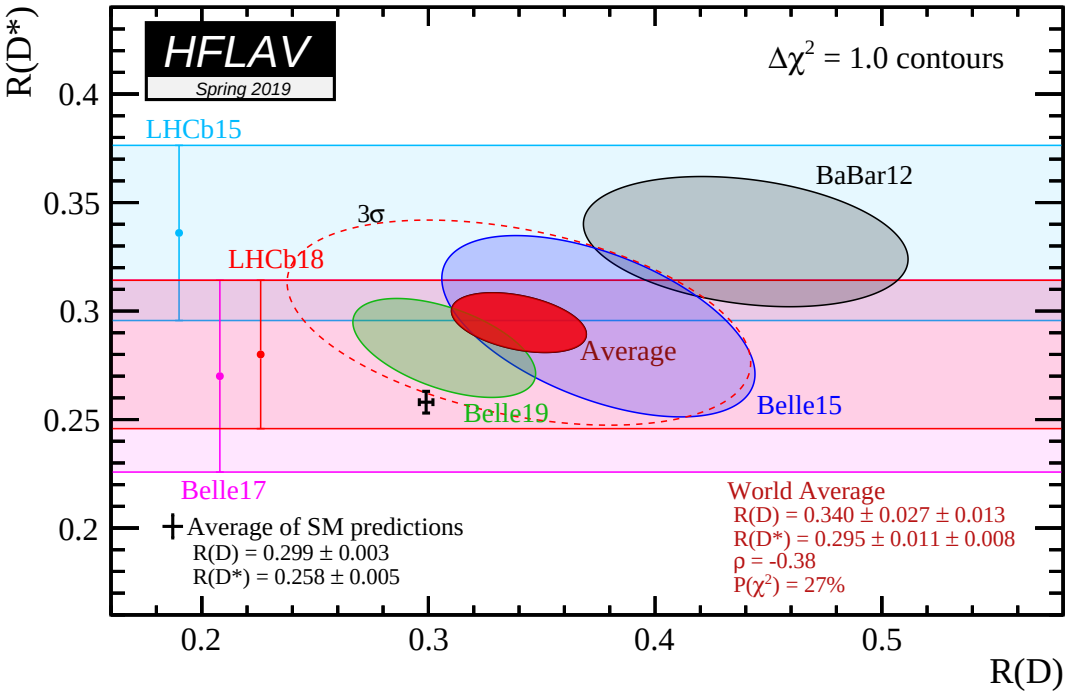


Figure 75.1: Measurements of $R(D)$ and $R(D^*)$ and their two-dimensional average compared with the average predictions for $R(D)$ and $R(D^*)$. Contours correspond to $\Delta\chi^2 = 1$ *i.e.*, 68% CL for the bands and 39% CL for the ellipses. The prediction and the experimental average deviate from each other by $3.08\sigma$. The dashed ellipse corresponds to a $3\sigma$ contour (99.73% CL).

## 75.6 Conclusion

The study of semileptonic $B$ meson decays continues to be an active area for both theory and experiment. The application of HQE calculations to inclusive decays is mature, and fits to moments of $\bar{B} \to X_c \ell \bar{\nu}_\ell$ decays provide precise values for $|V_{cb}|$ and, in conjunction with input on $m_c$ or from $B \to X_s \gamma$ decays, provide precise and consistent values for $m_b$.

The determination of $|V_{ub}|$ from inclusive $\bar{B} \to X_u \ell \bar{\nu}_\ell$ decays is based on multiple calculational approaches and independent measurements over a variety of kinematic regions, all of which provide consistent results. Further progress in this area is possible, but will require better theoretical control over higher-order terms, improved experimental knowledge of the $\bar{B} \to X_c \ell \bar{\nu}_\ell$ background and improvements to the modeling of the $\bar{B} \to X_u \ell \bar{\nu}_\ell$ signal distributions.

In both $b \to u$ and $b \to c$ exclusive channels there has been significant recent progress in lattice-QCD calculations, resulting in improved precision on both $|V_{ub}|$ and $|V_{cb}|$. These calculations now provide information on the form factors well away from the high $q^2$ region, allowing better use of experimental data. For $|V_{cb}|$ recent measurements have provided binned data for fitting form factors with reduced model dependence.

The values from the inclusive and exclusive determinations of $|V_{cb}|$ $|V_{ub}|$ are only marginally consistent. This is a long-standing puzzle, and the measurement of $|V_{ub}|/|V_{cb}|$ from LHCb based on $\Lambda_b^0$ decays does not simplify the picture.

Both $|V_{cb}|$ and $|V_{ub}|$ are indispensable inputs into unitarity triangle fits. In particular, knowing $|V_{ub}|$ with good precision allows a test of CKM unitarity in a most direct way, by comparing the length of the $|V_{ub}|$ side of the unitarity triangle with the measurement of $\sin(2\beta)$. This comparison of a "tree" process ($b \to u$) with a "loop-induced" process ($B^0 - \bar{B}^0$ mixing) provides sensitivity to

possible contributions from new physics.

The observation of semileptonic decays into $\tau$ leptons has opened a new window to the physics of the third generation. The measurements indicate a tension between the data and the Standard Model prediction, which could be a hint for new physics, manifesting itself as a violation of lepton universality beyond the standard-model couplings to the Higgs. It should be noted that none of the most recent measurements alone claim evidence for a deviation from the Standard Model. Combining the data of the semitauonic decays with the anomalies observed in the FCNC $b \to s\ell\ell$ transitions allows an interpretation in terms of additional $Z'$ or in terms of additional leptoquarks, but the current data does not allow us to draw a definite conclusion.

The authors would like to acknowledge helpful input from C. Bozzi, M. Rotondo, and C. Schwanda P. Gambino, Z. Ligeti, F. Bernlochner, S. Stone, S. Meinel, G. Wormser, and D. Robinson.

## References

[1] C. Patrignani *et al.* (Particle Data Group), Chin. Phys. **C40**, 10, 100001 (2016).

[2] See"Heavy-Quark and Soft-Collinear Effective Theory" by C.W. Bauer and M. Neubert in this *Review*.

[3] See "Lattice Quantum Chromodynamics" by S. Hashimoto, J. Laiho, and S.R. Sharpe in this *Review*.

[4] See "Production and Decay of b-Flavored Hadrons" by P. Eerola, M. Kreps and Y. Kwon in this *Review*.

[5] Y. S. Amhis *et al.* (HFLAV) (2019), [arXiv:1909.12524].

[6] N. Isgur and M. B. Wise, Phys. Lett. **B232**, 113 (1989); N. Isgur and M. B. Wise, Phys. Lett. **B237**, 527 (1990).

[7] M. A. Shifman and M. B. Voloshin, Sov. J. Nucl. Phys. **47**, 511 (1988), [Yad. Fiz.47,801(1988)].

[8] M. E. Luke, Phys. Lett. **B252**, 447 (1990).

[9] A. V. Manohar and M. B. Wise, Camb. Monogr. Part. Phys. Nucl. Phys. Cosmol. **10**, 1 (2000).

[10] H. Georgi, Phys. Lett. **B240**, 447 (1990).

[11] A. F. Falk *et al.*, Nucl. Phys. **B343**, 1 (1990).

[12] E. Eichten and B. R. Hill, Phys. Lett. **B234**, 511 (1990).

[13] A. Sirlin, Nucl. Phys. **B196**, 83 (1982).

[14] J. A. Bailey *et al.* (Fermilab Lattice, MILC), Phys. Rev. **D89**, 11, 114504 (2014), [arXiv:1403.0635].

[15] C. G. Boyd, B. Grinstein and R. F. Lebed, Phys. Rev. Lett. **74**, 4603 (1995), [hep-ph/9412324].

[16] C. G. Boyd, B. Grinstein and R. F. Lebed, Phys. Rev. **D56**, 6895 (1997), [hep-ph/9705252].

[17] B. Grinstein and A. Kobach, Phys. Lett. **B771**, 359 (2017), [arXiv:1703.08170].

[18] I. Caprini, L. Lellouch and M. Neubert, Nucl. Phys. **B530**, 153 (1998), [hep-ph/9712417].

[19] D. Bigi, P. Gambino and S. Schacht, Phys. Lett. **B769**, 441 (2017), [arXiv:1703.06124].

[20] P. Gambino, M. Jung and S. Schacht, Phys. Lett. **B795**, 386 (2019), [arXiv:1905.08209].

[21] F. U. Bernlochner, Z. Ligeti and D. J. Robinson, Phys. Rev. **D100**, 1, 013005 (2019), [arXiv:1902.09553].

[22] F. U. Bernlochner *et al.*, Phys. Rev. **D96**, 9, 091503 (2017), [arXiv:1708.07134].

[23] A. Czarnecki and K. Melnikov, Nucl. Phys. **B505**, 65 (1997), [hep-ph/9703277].

[24] J. Harrison, C. Davies and M. Wingate (HPQCD), Phys. Rev. **D97**, 5, 054502 (2018), [arXiv:1711.11013].

[25] S. Aoki *et al.* (Flavour Lattice Averaging Group) (2019), [arXiv:1902.08191].

[26] I. I. Y. Bigi *et al.*, Phys. Rev. **D52**, 196 (1995), [hep-ph/9405410].

[27] A. Kapustin *et al.*, Phys. Lett. **B375**, 327 (1996), [hep-ph/9602262].

[28] P. Gambino, T. Mannel and N. Uraltsev, Phys. Rev. **D81**, 113002 (2010), [arXiv:1004.2859].

[29] P. Gambino, T. Mannel and N. Uraltsev, JHEP **10**, 169 (2012), [arXiv:1206.2296].

[30] D. Buskulic *et al.* (ALEPH), Phys. Lett. **B395**, 373 (1997).

[31] G. Abbiendi *et al.* (OPAL), Phys. Lett. **B482**, 15 (2000), [hep-ex/0003013].

[32] P. Abreu *et al.* (DELPHI), Phys. Lett. **B510**, 55 (2001), [hep-ex/0104026].

[33] J. Abdallah *et al.* (DELPHI), Eur. Phys. J. **C33**, 213 (2004), [hep-ex/0401023].

[34] N. E. Adam *et al.* (CLEO), Phys. Rev. **D67**, 032001 (2003), [hep-ex/0210040].

[35] B. Aubert *et al.* (BaBar), Phys. Rev. **D77**, 032002 (2008), [arXiv:0705.4008].

[36] B. Aubert *et al.* (BaBar), Phys. Rev. Lett. **100**, 231803 (2008), [arXiv:0712.3493].

[37] B. Aubert *et al.* (BaBar), Phys. Rev. **D79**, 012002 (2009), [arXiv:0809.0828].

[38] W. Dungel *et al.* (Belle), Phys. Rev. **D82**, 112007 (2010), [arXiv:1010.5620].

[39] A. Abdesselam *et al.* (Belle) (2017), [arXiv:1702.01521].

[40] A. Abdesselam *et al.* (Belle) (2018), [arXiv:1809.03290].

[41] J. P. Lees *et al.* (BaBar), Phys. Rev. Lett. **123**, 091801 (2019), [arXiv:1903.10002].

[42] J. A. Bailey *et al.* (MILC), Phys. Rev. **D92**, 3, 034506 (2015), [arXiv:1503.07237].

[43] H. Na *et al.* (HPQCD), Phys. Rev. **D92**, 5, 054510 (2015), [Erratum: Phys. Rev.D93,no.11,119906(2016)], [arXiv:1505.03925].

[44] C. Bourrely, I. Caprini and L. Lellouch, Phys. Rev. **D79**, 013008 (2009), [Erratum: Phys. Rev.D82,099902(2010)], [arXiv:0807.2722].

[45] B. Aubert *et al.* (BaBar), Phys. Rev. Lett. **104**, 011802 (2010), [arXiv:0904.4063].

[46] R. Glattauer *et al.* (Belle), Phys. Rev. **D93**, 3, 032006 (2016), [arXiv:1510.03657].

[47] D. Bigi and P. Gambino, Phys. Rev. **D94**, 9, 094008 (2016), [arXiv:1606.08030].

[48] A. V. Manohar and M. B. Wise, Phys. Rev. **D49**, 1310 (1994), [hep-ph/9308246].

[49] I. I. Y. Bigi *et al.*, Phys. Rev. Lett. **71**, 496 (1993), [,201(1993)], [hep-ph/9304225]; I. I. Y. Bigi *et al.*, Phys. Lett. **B323**, 408 (1994), [hep-ph/9311339].

[50] D. Benson *et al.*, Nucl. Phys. **B665**, 367 (2003), [hep-ph/0302262].

[51] M. Gremm and A. Kapustin, Phys. Rev. **D55**, 6924 (1997), [hep-ph/9603448].

[52] B. M. Dassinger, T. Mannel and S. Turczyk, JHEP **03**, 087 (2007), [hep-ph/0611168].

[53] I. I. Bigi, N. Uraltsev and R. Zwicky, Eur. Phys. J. **C50**, 539 (2007), [hep-ph/0511158].

[54] T. Mannel, S. Turczyk and N. Uraltsev, JHEP **11**, 109 (2010), [arXiv:1009.4622].

[55] A. Pak and A. Czarnecki, Phys. Rev. **D78**, 114015 (2008), [arXiv:0808.3509].

[56] S. Biswas and K. Melnikov, JHEP **02**, 089 (2010), [arXiv:0911.4142].

[57] P. Gambino, JHEP **09**, 055 (2011), [arXiv:1107.3100].

[58] P. Gambino and N. Uraltsev, Eur. Phys. J. **C34**, 181 (2004), [hep-ph/0401063].

[59] V. Aquila *et al.*, Nucl. Phys. **B719**, 77 (2005), [hep-ph/0503083].

[60] T. Becher, H. Boos and E. Lunghi, JHEP **12**, 062 (2007), [arXiv:0708.0855].

[61] A. Alberti *et al.*, Nucl. Phys. **B870**, 16 (2013), [arXiv:1212.5082].

[62] A. Alberti, P. Gambino and S. Nandi, JHEP **01**, 147 (2014), [arXiv:1311.7381].

[63] T. Mannel, A. A. Pivovarov and D. Rosenthal, Phys. Rev. **D92**, 5, 054025 (2015), [arXiv:1506.08167].

[64] C. Breidenbach *et al.*, Phys. Rev. **D78**, 014022 (2008), [arXiv:0805.0971].

[65] I. Bigi *et al.*, JHEP **04**, 073 (2010), [arXiv:0911.3322].

[66] A. Kobach and S. Pal, Phys. Lett. **B772**, 225 (2017), [arXiv:1704.00008].

[67] J. Heinonen and T. Mannel, Nucl. Phys. **B889**, 46 (2014), [arXiv:1407.4384].

[68] P. Gambino, K. J. Healey and S. Turczyk, Phys. Lett. **B763**, 60 (2016), [arXiv:1606.06174].

[69] T. Mannel and K. K. Vos, JHEP **06**, 115 (2018), [arXiv:1802.09409].

[70] M. Fael, T. Mannel and K. Keri Vos, JHEP **02**, 177 (2019), [arXiv:1812.07472].

[71] I. I. Y. Bigi *et al.*, Phys. Rev. **D50**, 2234 (1994), [hep-ph/9402360].

[72] A. H. Hoang, Z. Ligeti and A. V. Manohar, Phys. Rev. Lett. **82**, 277 (1999), [hep-ph/9809423].

[73] A. H. Hoang, Z. Ligeti and A. V. Manohar, Phys. Rev. **D59**, 074017 (1999), [hep-ph/9811239].

[74] A. H. Hoang and T. Teubner, Phys. Rev. **D60**, 114027 (1999), [hep-ph/9904468].

[75] A. H. Hoang, Phys. Rev. **D61**, 034005 (2000), [hep-ph/9905550].

[76] S. E. Csorna *et al.* (CLEO), Phys. Rev. **D70**, 032002 (2004), [hep-ex/0403052].

[77] A. H. Mahmood *et al.* (CLEO), Phys. Rev. **D70**, 032003 (2004), [hep-ex/0403053].

[78] B. Aubert *et al.* (BaBar), Phys. Rev. **D69**, 111103 (2004), [hep-ex/0403031].

[79] B. Aubert *et al.* (BaBar), Phys. Rev. **D69**, 111104 (2004), [hep-ex/0403030].

[80] C. Schwanda *et al.* (Belle), Phys. Rev. **D75**, 032005 (2007), [hep-ex/0611044].

[81] P. Urquijo *et al.* (Belle), Phys. Rev. **D75**, 032001 (2007), [hep-ex/0610012].

[82] J. Abdallah *et al.* (DELPHI), Eur. Phys. J. **C45**, 35 (2006), [hep-ex/0510024].

[83] D. Acosta *et al.* (CDF), Phys. Rev. **D71**, 051103 (2005), [hep-ex/0502003].

[84] B. Aubert *et al.* (BaBar), Phys. Rev. **D81**, 032003 (2010), [arXiv:0908.0415].

[85] A. Limosani *et al.* (Belle), Phys. Rev. Lett. **103**, 241801 (2009), [arXiv:0907.1384].

[86] C. Schwanda *et al.* (Belle), Phys. Rev. **D78**, 032016 (2008), [arXiv:0803.2158].

[87] B. Aubert *et al.* (BaBar), Phys. Rev. **D72**, 052004 (2005), [hep-ex/0508004].

[88] B. Aubert *et al.* (BaBar), Phys. Rev. Lett. **97**, 171803 (2006), [hep-ex/0607071].

[89] S. Chen *et al.* (CLEO), Phys. Rev. Lett. **87**, 251807 (2001), [hep-ex/0108032].

[90] M. Battaglia *et al.*, eConf **C0304052**, WG102 (2003), [Phys. Lett.B556,41(2003)], [hep-ph/0210319].

[91] B. Aubert *et al.* (BaBar), Phys. Rev. Lett. **93**, 011803 (2004), [hep-ex/0404017].

[92] O. Buchmüller and H. Flächer, `hep-ph/0507253` updated in Ref. [219].

[93] C. W. Bauer *et al.*, Phys. Rev. **D70**, 094017 (2004), updated in Ref. [219], [hep-ph/0408002].

[94] P. Gambino and C. Schwanda, Phys. Rev. **D89**, 1, 014022 (2014), [arXiv:1307.4551].

[95] A. Alberti *et al.*, Phys. Rev. Lett. **114**, 6, 061802 (2015), [arXiv:1411.6560].

[96] M. Antonelli *et al.*, Phys. Rept. **494**, 197 (2010), see section 5.4.2, [arXiv:0907.5386].

[97] B. Dehnadi *et al.*, JHEP **09**, 103 (2013), [arXiv:1102.2264].

[98] I. Allison *et al.* (HPQCD), Phys. Rev. **D78**, 054513 (2008), [arXiv:0805.2999].

[99] K. G. Chetyrkin *et al.*, Phys. Rev. **D80**, 074010 (2009), [arXiv:0907.2110].

[100] N. Uraltsev, Int. J. Mod. Phys. **A14**, 4641 (1999), [hep-ph/9905520].

[101] M. Neubert, Phys. Rev. **D49**, 4623 (1994), [hep-ph/9312311]; M. Neubert, Phys. Rev. **D49**, 3392 (1994), [hep-ph/9311325].

[102] I. I. Y. Bigi *et al.*, Int. J. Mod. Phys. **A9**, 2467 (1994), [hep-ph/9312359].

[103] C. W. Bauer, M. E. Luke and T. Mannel, Phys. Rev. **D68**, 094001 (2003), [hep-ph/0102089].

[104] M. Benzke *et al.*, Phys. Rev. Lett. **106**, 141801 (2011), [arXiv:1012.3167].

[105] A. Gunawardana and G. Paz (2019), [arXiv:1908.02812].

[106] M. Neubert, Phys. Lett. **B513**, 88 (2001), [hep-ph/0104280].

[107] M. Neubert, Phys. Lett. **B543**, 269 (2002), [hep-ph/0207002].

[108] A. K. Leibovich, I. Low and I. Z. Rothstein, Phys. Rev. **D61**, 053006 (2000), [hep-ph/9909404].

[109] A. K. Leibovich, I. Low and I. Z. Rothstein, Phys. Rev. **D62**, 014010 (2000), [hep-ph/0001028].

[110] A. K. Leibovich, I. Low and I. Z. Rothstein, Phys. Lett. **B486**, 86 (2000), [hep-ph/0005124].

[111] A. K. Leibovich, I. Low and I. Z. Rothstein, Phys. Lett. **B513**, 83 (2001), [hep-ph/0105066].

[112] A. H. Hoang, Z. Ligeti and M. Luke, Phys. Rev. **D71**, 093007 (2005), [hep-ph/0502134].

[113] B. O. Lange, M. Neubert and G. Paz, JHEP **10**, 084 (2005), [hep-ph/0508178].

[114] B. O. Lange, JHEP **01**, 104 (2006), [hep-ph/0511098].

[115] M. Neubert, Phys. Lett. **B612**, 13 (2005), [hep-ph/0412241].

[116] Z. Ligeti, I. W. Stewart and F. J. Tackmann, Phys. Rev. **D78**, 114014 (2008), [arXiv:0807.1926].

[117] P. Gambino, K. J. Healey and C. Mondino, Phys. Rev. **D94**, 1, 014031 (2016), [arXiv:1604.07598].

[118] B. O. Lange, M. Neubert and G. Paz, Phys. Rev. **D72**, 073006 (2005), [hep-ph/0504071].

[119] P. Gambino *et al.*, JHEP **10**, 058 (2007), [arXiv:0707.2493].

[120] J. R. Andersen and E. Gardi, JHEP **01**, 097 (2006), [hep-ph/0509360].

[121] M. Beneke *et al.*, JHEP **06**, 071 (2005), [hep-ph/0411395].

[122] C. Greub, M. Neubert and B. D. Pecjak, Eur. Phys. J. **C65**, 501 (2010), [arXiv:0909.1609].

[123] M. Brucherseifer, F. Caola and K. Melnikov, Phys. Lett. **B721**, 107 (2013), [arXiv:1302.0444].

[124] T. Mannel and S. Recksiegel, Phys. Rev. **D60**, 114040 (1999), [hep-ph/9904475].

[125] U. Aglietti *et al.*, Eur. Phys. J. **C59**, 831 (2009), [arXiv:0711.0860].

[126] C. W. Bauer, Z. Ligeti and M. E. Luke, Phys. Rev. **D64**, 113004 (2001), [hep-ph/0107074].

[127] C. W. Bauer, Z. Ligeti and M. E. Luke, Phys. Lett. **B479**, 395 (2000), [hep-ph/0002161].

[128] I. I. Y. Bigi and N. G. Uraltsev, Nucl. Phys. **B423**, 33 (1994), [hep-ph/9310285].

[129] M. B. Voloshin, Phys. Lett. **B515**, 74 (2001), [hep-ph/0106040].

[130] Z. Ligeti, M. Luke and A. V. Manohar, Phys. Rev. **D82**, 033003 (2010), [arXiv:1003.1351].

[131] P. Gambino and J. F. Kamenik, Nucl. Phys. **B840**, 424 (2010), [arXiv:1004.0114].

[132] J. L. Rosner *et al.* (CLEO), Phys. Rev. Lett. **96**, 121801 (2006), [hep-ex/0601027].

[133] R. Barate *et al.* (ALEPH), Eur. Phys. J. **C6**, 555 (1999).

[134] M. Acciarri *et al.* (L3), Phys. Lett. **B436**, 174 (1998).

[135] G. Abbiendi *et al.* (OPAL), Eur. Phys. J. **C21**, 399 (2001), [hep-ex/0107016].

[136] P. Abreu *et al.* (DELPHI), Phys. Lett. **B478**, 14 (2000), [hep-ex/0105054].

[137] A. Bornheim *et al.* (CLEO), Phys. Rev. Lett. **88**, 231803 (2002), [hep-ex/0202019].

[138] A. Limosani *et al.* (Belle), Phys. Lett. **B621**, 28 (2005), [hep-ex/0504046].

[139] B. Aubert *et al.* (BaBar), Phys. Rev. **D73**, 012006 (2006), [hep-ex/0509040].

[140] J. P. Lees *et al.* (BaBar), Phys. Rev. **D95**, 7, 072001 (2017), [arXiv:1611.05624].

[141] B. Aubert *et al.* (BaBar), Phys. Rev. Lett. **95**, 111801 (2005), [Erratum: Phys. Rev. Lett.97,019903(2006)], [hep-ex/0506036].

[142] R. V. Kowalewski and S. Menke, Phys. Lett. **B541**, 29 (2002), [hep-ex/0205038].

[143] J. P. Lees *et al.* (BaBar), Phys. Rev. **D86**, 032004 (2012), [arXiv:1112.0702].

[144] I. Bizjak *et al.* (Belle), Phys. Rev. Lett. **95**, 241801 (2005), [hep-ex/0505088].

[145] P. Urquijo *et al.* (Belle), Phys. Rev. Lett. **104**, 021801 (2010), [arXiv:0907.0379].

[146] B. Aubert *et al.* (BaBar), Phys. Rev. Lett. **96**, 221801 (2006), [hep-ex/0601046].

[147] A. Sibidanov *et al.* (Belle), Phys. Rev. **D88**, 3, 032005 (2013), [arXiv:1306.2781].

[148] B. Aubert *et al.* (BaBar), Phys. Rev. Lett. **90**, 181801 (2003), [eConfC0304052,WG117(2003)], [hep-ex/0301001].

[149] T. Hokuue *et al.* (Belle), Phys. Lett. **B648**, 139 (2007), [hep-ex/0604024].

[150] B. Aubert *et al.* (BaBar), Phys. Rev. **D79**, 052011 (2009), [arXiv:0808.3524].

[151] J. P. Lees *et al.* (BaBar), Phys. Rev. **D88**, 7, 072006 (2013), [arXiv:1308.2589].

[152] J. P. Lees *et al.* (BaBar), Phys. Rev. **D87**, 3, 032004 (2013), [Erratum: Phys. Rev.D87,no.9,099904(2013)], [arXiv:1205.6245].

[153] C. Schwanda *et al.* (Belle), Phys. Rev. Lett. **93**, 131803 (2004), [hep-ex/0402023].

[154] N. E. Adam *et al.* (CLEO), Phys. Rev. Lett. **99**, 041802 (2007), [hep-ex/0703041].

[155] S. B. Athar *et al.* (CLEO), Phys. Rev. **D68**, 072003 (2003), superceded by Ref. [156], [hep-ex/0304019].

[156] R. Gray *et al.* (CLEO), Phys. Rev. **D76**, 012007 (2007), [Addendum: Phys. Rev.D76,no.3,039901(2007)], [hep-ex/0703042].

[157] P. del Amo Sanchez *et al.* (BaBar), Phys. Rev. **D83**, 032007 (2011), supercedes Ref. [158], [arXiv:1005.3288].

[158] B. Aubert *et al.* (BaBar), Phys. Rev. **D72**, 051102 (2005), [hep-ex/0507003].

[159] P. del Amo Sanchez *et al.* (BaBar), Phys. Rev. **D83**, 052011 (2011), updated in Ref. [160], [arXiv:1010.0987].

[160] J. P. Lees *et al.* (BaBar), Phys. Rev. **D86**, 092004 (2012), [arXiv:1208.1253].

[161] J. A. Bailey *et al.* (Fermilab Lattice, MILC), Phys. Rev. **D92**, 1, 014024 (2015), [arXiv:1503.07839].

[162] A. Bazavov *et al.* (Fermilab Lattice, MILC), Phys. Rev. **D100**, 3, 034501 (2019), [arXiv:1901.02561].

[163] C. M. Bouchard *et al.*, Phys. Rev. **D90**, 054506 (2014), [arXiv:1406.2279].

[164] B. Colquhoun *et al.*, Phys. Rev. **D93**, 3, 034502 (2016), [arXiv:1510.07446].
[165] J. M. Flynn *et al.*, Phys. Rev. **D91**, 7, 074510 (2015), [arXiv:1501.05373].
[166] T. Becher and R. J. Hill, Phys. Lett. **B633**, 61 (2006), [hep-ph/0509090].
[167] M. C. Arnesen *et al.*, Phys. Rev. Lett. **95**, 071802 (2005), [hep-ph/0504209].
[168] M. A. Shifman, A. I. Vainshtein and V. I. Zakharov, Nucl. Phys. **B147**, 385 (1979); M. A. Shifman, A. I. Vainshtein and V. I. Zakharov, Nucl. Phys. **B147**, 448 (1979).
[169] P. Ball and R. Zwicky, Phys. Rev. **D71**, 014015 (2005), [hep-ph/0406232].
[170] G. Duplancic *et al.*, JHEP **04**, 014 (2008), [arXiv:0801.1796].
[171] A. Bharucha, JHEP **05**, 092 (2012), [arXiv:1203.1359].
[172] A. V. Rusov, Eur. Phys. J. **C77**, 7, 442 (2017), [arXiv:1705.01929].
[173] I. Sentitemsu Imsong *et al.*, JHEP **02**, 126 (2015), [arXiv:1409.7816].
[174] H. Ha *et al.* (Belle), Phys. Rev. **D83**, 071101 (2011), [arXiv:1012.0090].
[175] B. Aubert *et al.* (BaBar), Phys. Rev. Lett. **101**, 081801 (2008), [arXiv:0805.2408].
[176] W. S. Brower and H. P. Paar, Nucl. Instrum. Meth. **A421**, 411 (1999), [hep-ex/9710029].
[177] P. Ball, eConf **C070512**, 016 (2007), [arXiv:0705.2290].
[178] J. M. Flynn and J. Nieves, Phys. Lett. **B649**, 269 (2007), [hep-ph/0703284].
[179] S. Aoki *et al.*, Eur. Phys. J. **C77**, 2, 112 (2017), [arXiv:1607.00299].
[180] T. Feldmann and M. W. Y. Yip, Phys. Rev. **D85**, 014035 (2012), [Erratum: Phys. Rev.D86,079901(2012)], [arXiv:1111.1844].
[181] W. Detmold, C. Lehner and S. Meinel, Phys. Rev. **D92**, 3, 034503 (2015), [arXiv:1503.01421].
[182] R. Aaij *et al.* (LHCb), Nature Phys. **11**, 743 (2015), [arXiv:1504.01568].
[183] M. Ablikim *et al.* (BESIII), Phys. Rev. Lett. **116**, 5, 052001 (2016), [arXiv:1511.08380].
[184] R. Aaij *et al.* (LHCb), Phys. Rev. **D96**, 11, 112005 (2017), [arXiv:1709.01920].
[185] M. Tanaka, Z. Phys. **C67**, 321 (1995), [hep-ph/9411405].
[186] H. Itoh, S. Komine and Y. Okada, Prog. Theor. Phys. **114**, 179 (2005), [hep-ph/0409228].
[187] U. Nierste, S. Trine and S. Westhoff, Phys. Rev. **D78**, 015006 (2008), [arXiv:0801.4938].
[188] M. Tanaka and R. Watanabe, Phys. Rev. **D82**, 034027 (2010), [arXiv:1005.4306].
[189] A. Datta, M. Duraisamy and D. Ghosh, Phys. Rev. **D86**, 034027 (2012), [arXiv:1206.3760].
[190] D. Bečirević, N. Košnik and A. Tayduganov, Phys. Lett. **B716**, 208 (2012), [arXiv:1206.4977].
[191] S. Fajfer *et al.*, Phys. Rev. Lett. **109**, 161801 (2012), [arXiv:1206.1872].
[192] A. Crivellin, C. Greub and A. Kokulu, Phys. Rev. **D86**, 054014 (2012), [arXiv:1206.2634].
[193] M. Bauer and M. Neubert, Phys. Rev. Lett. **116**, 14, 141802 (2016), [arXiv:1511.01900].
[194] I. Doršner *et al.*, Phys. Rept. **641**, 1 (2016), [arXiv:1603.04993].
[195] A. Celis *et al.*, Phys. Lett. **B771**, 168 (2017), [arXiv:1612.07757].
[196] J. F. Kamenik and F. Mescia, Phys. Rev. **D78**, 014003 (2008), [arXiv:0802.3790].
[197] S. Fajfer, J. F. Kamenik and I. Nisandzic, Phys. Rev. **D85**, 094025 (2012), [arXiv:1203.2654].
[198] M. Bordone, M. Jung and D. van Dyk (2019), [arXiv:1908.09398].
[199] B. Aubert *et al.* (BaBar), Phys. Rev. Lett. **100**, 021801 (2008), [arXiv:0709.1698].
[200] J. P. Lees *et al.* (BaBar), Phys. Rev. Lett. **109**, 101802 (2012), [arXiv:1205.5442].
[201] J. P. Lees *et al.* (BaBar), Phys. Rev. **D88**, 7, 072012 (2013), [arXiv:1303.0571].

[202] M. Huschle *et al.* (Belle), Phys. Rev. **D92**, 7, 072014 (2015), [arXiv:1507.03233].

[203] Y. Sato *et al.* (Belle), Phys. Rev. **D94**, 7, 072007 (2016), [arXiv:1607.07923].

[204] S. Hirose *et al.* (Belle), Phys. Rev. Lett. **118**, 21, 211801 (2017), [arXiv:1612.00529].

[205] G. Caria *et al.* (Belle) (2019), [arXiv:1910.05864].

[206] R. Aaij *et al.* (LHCb), Phys. Rev. Lett. **115**, 11, 111803 (2015), [Erratum: Phys. Rev. Lett.115,no.15,159901(2015)], [arXiv:1506.08614].

[207] R. Aaij *et al.* (LHCb), Phys. Rev. Lett. **120**, 17, 171802 (2018), [arXiv:1708.08856].

[208] `http://www.slac.stanford.edu/xorg/hfag/semi/fpcp17/RDRDs.html`.

[209] J. G. Korner and G. A. Schuler, Z. Phys. **C46**, 93 (1990).

[210] A. Abdesselam *et al.* (Belle), in "10th International Workshop on the CKM Unitarity Triangle (CKM 2018) Heidelberg, Germany, September 17-21, 2018," (2019), [arXiv:1903.03102].

[211] A. Matyja *et al.* (Belle), Phys. Rev. Lett. **99**, 191807 (2007), [arXiv:0706.4429].

[212] A. Bozek *et al.* (Belle), Phys. Rev. **D82**, 072005 (2010), [arXiv:1005.2302].

[213] M. Tanaka and R. Watanabe, Phys. Rev. **D87**, 3, 034028 (2013), [arXiv:1212.1878].

[214] R. Aaij *et al.* (LHCb), Phys. Rev. **D97**, 7, 072013 (2018), [arXiv:1711.02505].

[215] R. Aaij *et al.* (LHCb), Phys. Rev. Lett. **120**, 12, 121801 (2018), [arXiv:1711.05623].

[216] S. Hirose *et al.* (Belle), Phys. Rev. **D97**, 1, 012004 (2018), [arXiv:1709.00129].

[217] F. U. Bernlochner *et al.*, Phys. Rev. **D95**, 11, 115008 (2017), [erratum: Phys. Rev.D97,no.5,059902(2018)], [arXiv:1703.05330].

[218] S. Jaiswal, S. Nandi and S. K. Patra, JHEP **12**, 060 (2017), [arXiv:1707.09977].

[219] Y. Amhis *et al.* (HFLAV), Eur. Phys. J. **C77**, 12, 895 (2017), [arXiv:1612.07233].